INORGANIC CHEMISTRY FRONTIERS

REVIEW

View Article Online
View Journal | View Issue

Cite this: *Inorg. Chem. Front.*, 2020, **7**, 1082

Zn(II)/Cd(II) based mixed ligand coordination polymers as fluorosensors for aqueous phase detection of hazardous pollutants

Bhavesh Parmar,[a,b] Kamal Kumar Bisht,[c] Yadagiri Rachuri †[a,b] and Eringathodi Suresh *[a,b]

Environmental remediation, particularly in the context of water pollution, has been at the centre of a range of research domains over the past few decades. Metal organic frameworks (MOFs) or coordination polymers (CPs) are a relatively new class of infinite materials comprising metal nodes and linkers as repeat units. Exclusive merits of these materials such as tuneable porosity, and physical and chemical properties reflect in their extensive applications in fields such as sensing, adsorption, separation, catalysis, *etc*. In the present study, we evaluate the application of Zn(II)/Cd(II) based mixed ligand luminescent MOFs/CPs towards addressing the concerns related to water pollution. Firstly, the origin of photoluminescence in MOFs/CPs is discussed, which underlines the merits of Zn(II) and Cd(II) metal ions, mixed linker systems as well as the delicate host–guest interactions between the framework and analyte. The hydrolytic and chemical stability of the luminescent MOFs/CPs is prerequisite for their in-field sensing applications, which are critically studied in the context of Cd(II)/Zn(II) and mixed linker based luminescent MOFs/CPs. Subsequent sections separately underscore the important studies on sensing of organic pollutants *viz.*, nitroaromatics, acetone, acetylacetone and paraquat as well as inorganic pollutants including di- and trivalent metal cations *viz*, Hg^{2+}, Cu^{2+}, Pb^{2+}, Pd^{2+}, Al^{3+}, Fe^{3+} and Cr^{3+}; and inorganic anions such as cyanide, iodide, chromate, dichromate, manganate *etc*. Efforts to develop paper strip based versatile sensors for noxious ions are also highlighted.

Received 28th November 2019,
Accepted 4th January 2020

DOI: 10.1039/c9qi01549c

rsc.li/frontiers-inorganic

Introduction

Over the past few decades, growing attention has been paid to environmental issues, and one of the major challenges is the problem related to the chemical pollutants from industries and other sources. Among a range of water pollutants, nitroorganics, volatile organic compounds (VOCs), and ionic species of different chemicals are of major concern because they are noxious and have human health and environment-related implications. Particularly, many organic nitro compounds and organic solvents are used in many industries, and their eventual discharge into the wastewater leads to environmental problems and adverse effects to aquatic bodies. Hence, the detection and sensing of the mentioned hazardous chemicals, as well as their containment, have remained urgent issues over the past several years. Among the available methods, fluorescent sensors owing to their high sensitivity, fast response, and user-friendly operation have attracted extensive research interest in recent years. On the other hand, chromatographic and other spectroscopic methods used as detection tools are cumbersome and inefficient due to a longer processing time, low sensitivity, and high operational cost. Hence, the development of novel sensor materials with a simple and lucid strategy for the selective and judicious detection of trace levels of pollutants is obligatory to avoid the risk of toxicity.[1–10]

So far, there has been considerable progress towards the development of sensors for organic and inorganic pollutants using a variety of materials such as metal organic frameworks (MOF) or coordination polymers (CP), small organic probes, oligomers, nanomaterials, linear conjugated polymers, *etc*. Luminescent metal organic frameworks (LMOFs) or luminescent coordination polymers (LCPs) have emerged as potential sensor materials owing to their structural diversity, tailorable pore size, and thermal and chemical stabilities. Notably,

[a]*Analytical and Environmental Science Division and Centralized Instrument Facility, CSIR-Central Salt and Marine Chemicals Research Institute, G. B. Marg, Bhavnagar 364 002, Gujarat, India. E-mail: esuresh@csmcri.res.in, sureshe123@rediffmail.com*
[b]*Academy of Scientific and Innovative Research (AcSIR), Ghaziabad-201 002, India*
[c]*Department of Chemistry, RCU Government Post Graduate College, Uttarkashi-249193, Uttarakhand, India*
† Current address: KAUST Catalysis Center, King Abdullah University of Science and Technology, Thuwal 23955-6900, Saudi Arabia.

LMOFs or LCPs incorporating functional linkers and d^{10} or Ln metal nodes can be developed as fluorescent sensors. In fact, characteristic luminescence features of LMOFs/LCPs can be modulated by judicious combinations of metal nodes and the linker features such as spacer length, steric hindrance, π-electron availability, and conjugation and the working principle of LCPs as sensors is based on the photoluminescence properties which arise upon the relaxation of the electrons from the excited state to the ground state with photon emission. In sensing application, supramolecular interactions of LCPs with the analyte could increase or decrease the luminescence emission leading to the turn-on or turn-off display respectively.[11–21]

The detection of hazardous pollutants by LCPs has often been investigated in organic solvents. The scarcity of aqueous phase detection studies may be associated with the lack of chemical stability of LCPs in water or in the presence of analytes of interest. Hence, the chemical and hydrolytic stability of LCPs/MOFs remains a prerequisite for in-field application towards sensing of noxious analytes. Notably, several strategies to improve the water stability of MOFs/CPs have been reviewed recently.[22,23] There have been a few reviews referring to the designed synthesis of LCPs involving a single ligand moiety for the detection of nitroaromatics (NACs) and organic/inorganic pollutants in organic media.[1–3,15–18,21] Herein, we present recent developments in the fabrication of hydrolytically stable Zn(II)/Cd(II) based LCPs using a dual ligand strategy. A summary of the updated literature on the utilization of LCP materials for the aqueous phase detection of organic/inorganic pollutants has been presented in tabulated forms, and significant contributions in the selected research field have been discussed. We have mainly focused on the utilisation of the mixed ligand Zn(II)/Cd(II) based LCPs/LMOFs for the aqueous phase detection of organic pollutants (NACs/hazardous organic solvents) and hazardous cationic metal ions (*viz.*, Pb^{+2}, Hg^{+2}, Fe^{+3}, Pd^{+2}, Cr^{3+} *etc.*) and anionic species such as CrO_4^{2-}, $Cr_2O_7^{2-}$, MnO_4^-, CN^-, I^-, *etc.*

Photoluminescence and origin of luminescence in LCPs

The emission of light producing from the excited states upon the absorption of energy is termed luminescence. Generally, two types of luminescence called fluorescence and phosphorescence have been observed by radiative relaxation from the excited states accompanying the emission of photons. Fluorescence is a spin-allowed transition in which the light emission occurs between the energy states of the same spin multiplicity between the excited electronic state (S_1) and the ground state (S_0) with lifetimes in a nanosecond range. However, in the case of phosphorescence light emission occurs between states with different spin multiplicities in which transition occurs from a lowest excited triplet electronic state (T_1) to the ground state (S_0). This forbidden electronic transition slows down the emission process resulting in the lifetimes in the range of microseconds to few seconds.[24–26] The use of fluorescent bridging ligands such as aromatic conjugated moiety, photoactive metal ions or combination of both allows the generation of luminescence properties in CPs/MOFs. The encapsulated guest molecules in porous cavities of certain CPs also contribute to the luminescence properties. Hence, the observed luminescence signal in CPs demands consideration of all the photophysical transitions. Generally, luminescence in LCPs/LMOFs arises from the building blocks such as conjugated organic ligands or metal cations/clusters

Bhavesh Parmar

Bhavesh Parmar was born in Junagadh, Gujarat, India. He obtained his Masters (2012) in Chemistry from the Department of Chemistry, Saurashtra University. He subsequently joined the research group of Dr E. Suresh at CSIR-CSMCRI and is pursuing his doctoral work in the area of structural and functional features of multidimensional coordination polymers. His main area of research interest is the design and synthesis of multidimensional coordination polymers/metal–organic frameworks and their functional aspects such as photoluminescence sensing of organic/inorganic pollutants, CO_2 utilization of value-added chemicals and heterogeneous catalysis. While working with Dr E. Suresh, he also gained knowledge and experience in small molecule crystallography.

Kamal Kumar Bisht

Dr Kamal Kumar Bisht was born (1984) in Gangolihat, Uttarakhand, India. He obtained his Masters from Govt PG College, Pithoragarh in 2006 and subsequently joined the research group of Dr E. Suresh at CSIR-CSMCRI and obtained his PhD in 2014 for the design and synthesis of coordination polymers. He joined UPES, Dehradun as Assistant Professor in 2014 and two years later moved to RCU Govt PG College, Uttarkashi through UKPSC. He was recognized by RSC Chem. Soc. Rev. as one of the outstanding reviewers for the journal in 2016 and has been an affiliate of IUPAC since 2018. His research interests lie in CPs, MOFs, hybrid materials and environmental remediation. He presently has around 40 research articles and book chapters to his credit.

as mentioned above. Organic linkers with aromatic moieties or extended π systems are commonly used for the design and synthesis of CPs due to their rigid molecular backbone. The stacking of the adjacent linkers with an electron rich π cloud can contribute to luminescence and can be classified as linker-based luminescence or LLCT. Close proximity of the confined organic luminophores with well-ordered alignment in MOFs and their intermolecular interaction can alter the luminescence properties compared to the free one. Furthermore, a functionally decorated ligand moiety as a linker in CP/MOF has a tendency to involve supramolecular interaction with the guest molecule and has a profound effect in changing the emission properties of the pristine ligand moiety. A sensible choice of the metal ion/cluster nodes present in the CP/MOF can also lead to a photoactive building unit that enhances the luminescence properties. Particularly, the confinement of conjugated ligands in combination with transition metal ions (d^{10}) or lanthanide metal ions generates luminescence in CPs and can be designated as luminescent coordination polymers (LCPs), a subclass of CPs. π electron rich aromatic or conjugated ligand moieties by absorbing the radiative excitation energy and d^{10}/lanthanide metal cations in these hybrid materials are capable of stimulating luminescence emission in LCPs. Electronic properties such as optical absorption and emissions of LCPs can be tuned and have a direct correlation with the band gap. Thus, band gaps can be varied by changing the size of the SBU and the degree of conjugation of the organic linkers having the same metal center and network connectivity or changes to a framework's metal centers leading to atomic compositions of the valence band (or HOMO) and/or conduction band (or LUMO) which directly relates the fluorescence properties of LCPs.[24–33]

As mentioned before and previous reports revealed that metal ions/clusters, organic linker moieties, metal–organic charge transfer and guest molecules within porous/non-porous CPs/MOFs all can contribute towards luminescence through a variety of mechanisms. For example, in ligand-centred emission both photon absorption and emission processes occur on the same organic ligand as well as in separate locations within the framework through non-radiative energy and electron transfer processes enlightened by Förster–Dexter theory bridging the gap. The various active mechanisms behind the luminescence stimulation in CPs can be classified into ligand-to-ligand charge transfer (LLCT), ligand-to-metal charge transfer (LMCT), metal-to-ligand charge transfer (MLCT), metal-to-metal charge transfer (MMCT) and guest centred emission and guest-sensitization mechanisms. In the case of CPs/MOFs with paramagnetic transition metal having unpaired electrons ligand-field transitions (d–d transition) may lead to strong reabsorption and/or quenching of luminescence generated from the organic molecule which can occur *via* electron or energy transfer through the partially filled d-orbitals. However, paramagnetic metal such as Cu^{2+} based MOFs comprising a π conjugated pentiptycene based ligand showed strong emission under blue light (UV range). Particularly, d^{10} metal centres (Zn^{2+}/Cd^{2+} and Cu^{+}/Ag^{+}) are well known for the ligand centred

Yadagiri Rachuri

Dr Yadagiri Rachuri obtained his BSc from Osmania University and Masters from the Department of Chemistry, Pondicherry University. He joined the research group of Dr E. Suresh at CSIR-CSMCRI in 2012 as a junior research fellow (JRF) and received his Ph.D. on the synthesis, crystal structure and applications of multidimensional coordination polymers in 2018. Subsequently, he had been to South Korea and carried out his first post-doc at Pusan National University under the supervision of Prof. Dae-Won Park on MOFs as heterogeneous catalysts for the conversion of CO_2 to cyclic carbonates. Recently, he moved to the King Abdullah University of Science and Technology (KAUST), KSA and is currently pursuing his post-doctoral research with Prof. Kuo-Wei-Huang at the KAUST Catalysis Centre. His research interest focuses on the design and synthesis of metal organic frameworks (MOFs), covalent organic frameworks (COFs) and pincer complexes based on porous organic polymers as heterogeneous catalysts for CO_2 conversion and dehydrogenation of formic acid.

Eringathodi Suresh

Dr Eringathodi Suresh received his Ph.D. degree from Maharaja Krishnakumarsinhji Bhavnagar University, Gujarat, India for his work on synthesis and X-ray crystallographic studies on coordination polymers executed at CSIR-CSMCRI, under the guidance of Dr Mohan Bhadbhde. Upon completion of his PhD, he was awarded JSPS postdoctoral fellowship and worked with Prof. Katsuya Inoue, at the Institute of Molecular Science, Okazaki, Japan. He is also the recipient of a CSIR-DAAD fellowship for senior scientists and collaborated with Prof. Christof Wöll at the Karlsruhe Institute of Technology. For the last two decades, he has been working at CSIR-CSMCRI and continuing as a Senior Principal Scientist. The research focus of his team is on the design and synthesis of novel mixed ligand functional coordination polymers for chemical sensing, heterogeneous catalysis and also some basic aspects of chiral coordination polymers.

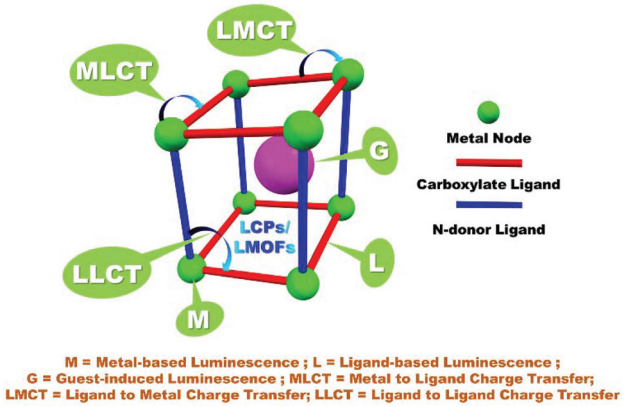

Scheme 1 Schematic representation for various pathways of luminescence origin in LCPs/LMOFs.[18,58]

transitions. Completely filled d-orbitals of metals and organic ligands are involved in two types of charge transfer namely ligand to metal charge transfer (LMCT) and metal to ligand charge transfer (MLCT). LMCT is often observed in Zn^{2+} and Cd^{2+} complexes, while MLCT is commonly present in Cu^{+} and Ag^{+} compounds. Interestingly, metal-centred luminescence is often observed when lanthanide/actinide metal nodes are assembled with conjugated organic linkers in the rigid MOF system. Luminescence in lanthanide-based LCPs is accounted for by the delivery of excitation energy through an antenna effect from the triplet excited states to the emissive states in lanthanides by strong photon absorbing ligands with efficient intersystem crossing (ISC).[24–26,34–43] To enliven the luminescence in the CP/MOF, aromatic di or polycarboxylate with a rigid backbone along with imidazole/pyridine ligands has been commonly used and explored for various applications including the detection of nitroorganic compounds. The various aspects and effects contributing to the luminescence in CPs/MOFs have been schematically demonstrated in Scheme 1.

LCPs as a prospective aqueous phase fluorosensor

π-Electron-rich luminescent organic molecules and polymers are commonly used for sensing hazardous molecules by turn on/turn off fluorescence behaviour. However, the multi-step synthetic protocol and lack of porous nature, recyclability and chemical stability of these materials are some shortcomings. LCPs have numerous key advantages over other potential luminescent probes. The tuneable nature of fluorescence properties by the prudent choice of the metal nodes and conjugated organic linkers and porosity of the inorganic–organic hybrid materials uses LCPs for sensing applications. The crystalline nature of LCPs shows a precise crystal structure by SXRD analysis with exact knowledge of the atomic position and their supramolecular interaction can give insight into the detection of analytes and the chemical stability of these materials offer an added advantage. Porosity in LCPs can provide easy access to the analytes increasing the interaction between the analytes and framework enhancing the sensing ability. The porous environment of the MOFs such as hydrophobicity, polarizability, polarity, acidity and proton affinity can be finely tuned by various chemical manipulations to suit the guest molecules. By tailoring the pore environment sensitive and selective capture of the targeted analytes can be achieved. It is also demonstrated that the functionalization of the pore channels by photochromic or conjugated organic ligands and post-synthetic modification in LCPs can improve the analyte detection. Permanent porosity and cooperative luminescence properties are particularly useful in the development of luminescence sensing materials including LCPs for a variety of sensing applications. The chemical sensors based on LCPs have drawn immense attention for their significant advantages, including short response time, high sensitivity and selectivity and reusability.[24–26,32,33]

Good emission properties, tunability of the framework topology and viability of selective supramolecular host–guest interactions between frameworks and target analytes are important assets of LCPs towards the detection of trace amounts of hazardous molecules including NACs. Sensing applications by LCPs in the organic/non-aqueous phase are well documented in the literature, but detection remains scantly explored in water may be due to the chemical instability of LCPs in aqueous media.[44–54] Since most of the MOFs are hydrophilic in nature the hydrolytic stability of these materials is a major concern for the practical implementation of these materials including sensing application. It is worth mentioning here the studies on the relative stability of notable MOFs in water and humid environments by Kaskel, and Matzger *et al.* followed by a few reports providing insight into the development of MOFs with hydrolytic stability and their aqueous phase sensing application.[55,56] A recent comprehensive review by Walton *et al.* clearly validated the progress in the design strategy and structural features of water stable MOFs.[22] Coordinatively saturated metal nodes/metal clusters and the presence of a hydrophobic ligand moiety can resist the approach of water molecules towards the coordination sphere imparting hydrolytic stability in LCPs. Considering the environmental issues and human health it is mandatory to develop new user-friendly materials such as LCPs as fluorosensors with good aqueous phase stability for practical utility in the detection of various hazardous analytes including explosives.

Functional aspects: sensing and detection of pollutants by LCPs

Organic pollutants

Water contamination and environmental problems have become major issues, as large volumes of effluents with high concentrations of toxic organic pollutants are being discharged into water bodies as a result of industrialization and

modern living. Governments and research groups all over the world are actively engaged in the remediation of organic waste water pollution and billions have been disbursed towards environmental protection. The detection of toxic organic pollutants such as different organic precursors and solvents used in the synthesis of value-added products, dyes, nitroaromatic compounds (NACs) *etc.* has always been an important challenge *vis-à-vis* environmental protection, human health, homeland security, and safety. For example, ketones are important raw materials which have been widely used in industrial production and their toxicity is a substantial threat to human health.[57–61]

On the other hand, amines are important precursors in chemical industry; 4-nitroaniline (4-NA) is one of the integral chemicals utilized in the synthesis of azo dyes, pesticides, pharmaceuticals, photostabilizers, *etc.* and their accumulation in water and soil can cause health problems such as respiratory arrest, diarrhoea, skin eczema, and anaemia. Aniline based compound, 2,6-dichloro-4-nitroaniline, is a pesticide used to control diseases in fruits, vegetables and crops and is harmful to human health as well.[62,63] Another class of compounds, nitro-aromatic compounds (NACs), which include 2,4,6-trinitrophenol (TNP), trinitrotoluene (TNT), 2,4-dinitrophenol (2,4-DNP), dinitrotoluene (DNT), *p*-nitrophenol (4-NP), 1,3-dinitrobenzene (1,3-DNB), nitrotoluene (NT), and nitrobenzene (NB), are not only strong explosives but also used extensively as raw materials in dyes, fireworks, and the pharmaceutical and leather industries.[15–18] Furthermore, improper disposal of these pollutants causes soil as well as aquatic pollutions and efficient and selective detection of these harmful chemicals in the aqueous phase is a challenge. Hence, the development of luminescent MOFs (LMOFs) with sensing properties has influenced researchers in detecting the toxic environmental contaminants. Luminescence-based detection has gained attention in recent years due to its user-friendly methodology, good sensitivity, quick response time and easy portability. The sensing mechanism mainly relies on electron rich LCPs that undergo quenching on interactions with the electron deficient analyte molecules especially in the case of NACs. This section comprises sensing and detection of various organic pollutants which include mainly different nitroaromatic compounds (NACs), organic solvents such as acetone, acetylacetone, *etc.* and herbicide/antibiotic molecules such as paraquat and nitrofurazone (NZF) using Zn(II)/Cd(II) mixed ligand LMOFs in water. A comprehensive survey on the sensing and detection of organic pollutants in water medium, which mainly include NACs using Zn(II)/Cd(II) mixed ligand coordination polymers as fluorosensors is summarised in Table 1.

TNP sensing in the aqueous phase by a dual ligand 3D MOF $\{[Zn_8(ad)_4(BPDC)_6O{\cdot}2Me_2NH_2]{\cdot}G\}_n$ (**1**) also identified as bio-MOF-1 containing BPDC (biphenyl dicarboxylic acid) and ad (adenine) as a fluorosensor has been reported by Ghosh *et al.* Water stable (**1**) shows tremendous selectivity and sensitivity for TNP among other NACs with K_{sv} value 4.60×10^4 M^{-1} and limit of detection (LOD) value 1.29×10^{-8} M. Free amino functionality on the adenine linker is highly influencing the sensitivity of (**1**) for TNP which is further supported by adenine-TNP co-crystal generation.[64] A mixed linker two-dimensional luminescent coordination polymer $[Cd(ppvppa)(1,4\text{-NDC})]_n$ (**2**) (where ppvppa = *N*-(pyridin-2-yl)-*N*-(4-(2-(pyridin-4-yl)vinyl)phenyl)pyridin-2-amine; 1,4-NDC = 1,4-naphthalenedicarboxylic acid) reported by Lang *et al.* shows selective sensing of 2,4-DNP with good recyclability. The luminescence of compound (**2**) is ppvppa ligand centric and offers blue fluorescence in the solid-state as well in different organic solvents including water. Quenching properties vary in the range of 91–72% for 2,4-DNP, 4-NP, and 4-NA with 2,4-DNP showing the highest quenching among different pools of NACs with K_{sv} value 1.18×10^2 M^{-1}.[65] In another report by Ghosh and co-workers, the synthesis and sensing application of $[Zn_4(DMF)(Ur)_2(NDC)_4]_n$ (**3**) composed of π-electron rich naphthalene carboxylate (NDC) and urotropine (Ur) ligands was demonstrated. A tertiary amine decorated porous MOF (**3**) showed excellent fluorescence properties in water and selectively detected explosive molecule TNP from a variety of NACs with K_{sv} 1.08×10^5 M^{-1} and LOD 7.10×10^{-6} M respectively. Interaction of the TNP hydroxyl group with an aliphatic amine on Ur also identified in the TNP-Ur co-crystal is one of the reasons behind the accurate detection of TNP *via* the energy transfer process (Fig. 1).[66] Similarly Su *et al.* reported a self-penetrating 3D chiral coordination polymer $\{[Cd(NDC)(L_1)]_2{\cdot}H_2O\}_n$ (**4**) (where L_1 = 4-amino-3,5-bis(4-imidazol-1-ylphenyl)-1,2,4-triazole) with good fluorescent properties. The crystal structure indicates helical chains in chiral CP (**4**) generated by a V-shaped N-donor linker L_1, which also contains an uncoordinated N-atom and amino functionality.

The luminescence properties of amino-functionalized (**4**) in water were successfully utilized for the selective and recyclable sensing of TNP with K_{sv} value 3.70×10^4 M^{-1} and the proposed sensing mechanism involves the combination of photoinduced electron-transfer (PET) and resonance energy transfer (RET) processes.[67] Zhang *et al.* reported the photoluminescence sensing of various nitro derivatives NB, 4-NA, 2-M-4-NA and 4-NP using 3D Cd(II) MOF $\{[Cd(5\text{-asba})(bimbu)]\}_n$ (**5**) constructed from multifunctional 2-amino-5-sulfobenzoic acid (5-asba) and N-donor linker (bimbu). Multi-responsive (**5**) detects NACs with very good quenching constant values 1.60×10^4 M^{-1} for NB, 9.80×10^4 M^{-1} for 4-NA, 8.10×10^4 M^{-1} for 2-M-4-NA and 6.10×10^4 M^{-1} for 4-NP in water suspension.[68] Versatile synthesis of acyl amide decorated isostructural two 3D Zn(II)/Cd(II) coordination polymers reported by our group exhibits water stability and photoluminescence properties. Both mixed linker LCPs, $\{[M(BDC)(L_2)]{\cdot}xG\}_n$, comprising Zn^{2+} (**6**) or Cd^{2+} (**7**), benzene-1,4-dicarboxylic acid (BDC) and N-donor ligand 4-pyridyl carboxaldehyde isonicotinoylhydrazone (L_2) cover a 2-fold interpenetrated pillared layered *pcu* topology. Florescence quenching performance in water towards TNP among different pools of NACs showed good selectivity and sensitivity with K_{sv} values 1.16×10^4 M^{-1} and 1.35×10^4 M^{-1} and limit of detection values 3.60×10^{-5} M and 1.50×10^{-5} M for (**6**) and (**7**) respectively. In addition to the PET and RET mechanism, quenching behaviour is also supplemented by H-bonding interaction between the amide group

Table 1 List of Zn(II)/Cd(II) mixed ligand LCP/LMOF sensors for aqueous-phase detection of organic pollutants

Sr no.	LCPs/LMOFs[a]	Organic analyte	K_{sv} (M^{-1})	LOD (M)	Ref.
1	$\{[Zn_8(ad)_4(BPDC)_6O\cdot 2Me_2NH_2]\cdot G\}_n$ (**1**)	TNP	4.60×10^4	1.29×10^{-8}	64
2	$[Cd(ppvppa)(1,4\text{-}NDC)]_n$ (**2**)	2,4-DNP	1.18×10^2	—	65
3	$[Zn_4(DMF)(Ur)_2(NDC)_4]_n$ (**3**)	TNP	1.08×10^5	7.10×10^{-6}	66
4	$\{[Cd(NDC)(L_1)]_2\cdot H_2O\}_n$ (**4**)	TNP	3.70×10^4	—	67
5	$\{[Cd(5\text{-}asba)(bimbu)]\}_n$ (**5**)	NB	1.60×10^4	—	68
		4-NA	9.80×10^4	—	
		2-M-4-NA	8.10×10^4	—	
		4-NP	6.10×10^4	—	
6	$\{[Zn(BDC)(L_2)]\cdot xG\}_n$ (**6**)	TNP	1.16×10^4	3.60×10^{-5}	69
	$\{[Cd(BDC)(L_2)]\cdot xG\}_n$ (**7**)	TNP	1.35×10^4	1.50×10^{-5}	
7	$[Cd(5\text{-}BrIP)(TIB)]_n$ (**8**)	TNP	2.68×10^4	2.70×10^{-5}	70
8	$\{[Cd_2(tib)_2(bda)_2]\cdot G\}_n$ (**9**)	Acetone	—	—	71
9	$\{[Zn_2(L_3)_2(bpy)]\cdot(DMF)\cdot(H_2O)_2\}_n$ (**10**)	TNP	1.53×10^4	3.48×10^{-6}	72
	$\{[Zn_2(L_3)_2(azp)]\cdot(DMF)_2\cdot(H_2O)\}_n$ (**11**)	TNP	3.11×10^4	1.82×10^{-6}	
10	$\{Zn_2(H_2L_5)_2(bpy)_2(H_2O)_3\cdot H_2O\}_n$ (**12**)	TNP	1.36×10^4	4.9×10^{-5}	73
11	$[Zn(\mu_2\text{-}1Had)(\mu_2\text{-}SO_4)]_n$ (**13**)	TNP	3.14×10^4	4.00×10^{-10}	74
12	$\{[Zn_3(L_6)_3(Ur)_2]\cdot 2DMF\cdot 3H_2O\}_n$ (**14**)	TNP	5.10×10^4	8.46×10^{-6}	75
13	$\{Zn_2(tpbn)(2,6\text{-}NDC)_2\}_n$ (**15**)	TNP	5.90×10^3	4.75×10^{-5}	76
	$\{[Zn_2(tphn)(2,6\text{-}NDC)2]\cdot 4H_2O\}_n$ (**16**)	TNP	2.46×10^3	8.11×10^{-5}	
14	$\{[Zn(IPA)(L_7)]\}_n$ (**17**)	TNP	2.16×10^4	1.20×10^{-7}	77
	$\{[Cd(IPA)(L_7)]\}_n$ (**18**)	TNP	1.52×10^4	6.00×10^{-8}	
15	$\{Zn_4(TPOM)(1,4\text{-}NDC)_4\}_n$ (**19**)	4-NA	7.87×10^4	6.40×10^{-7}	78
		2,6-DCNA	2.74×10^4	1.39×10^{-6}	
16	$[Cd(L_8)(IPA)]_n$ (**20**)	4-NP	1.86×10^4	—	79
	$\{[Zn_2(L_8)(L_3)_2]\cdot 3H_2O\}_n$ (**21**)	TNP	4.19×10^4	6.90×10^{-5}	
		4-NP	2.93×10^4	—	
	$\{Cd(L_8)(PDA)(H_2O)_2\}_n$ (**22**)	4-NP	1.89×10^4	—	
	$\{[Cd_3(L_8)(CHD)_3(DMF)_2]\cdot 2DMF\}_n$ (**23**)	4-NP	3.11×10^4	—	
17	$\{[Zn_2(Py_2TTz)_2(BDC)_2]\cdot 2(DMF)\cdot 0.5(H_2O)\}_n$ (**24**)	TNP	3.25×10^4	9.30×10^{-5}	80
		NZF	1.72×10^4	9.10×10^{-5}	
	$\{[Cd_2(Py_2TTz)_2(BDC)_2]\cdot 2(DMF)\}_n$ (**25**)	TNP	4.06×10^4	9.00×10^{-5}	
		NZF	4.53×10^4	8.50×10^{-5}	
18	$\{[Cd_3(SDB)_3(TIB)](H_2O)_2(1,4\text{-dioxane})(G)_x\}_n$ (**26**)	TNP	2.43×10^4	1.50×10^{-5}	81
19	$\{Zn(L_9)(L_3)(H_2O)\}_n$ (**27**)	TNP	—	—	82
	$\{Zn(L_9)(IPA)(DMF)(H_2O)_{1.5}\}_n$ (**28**)	NZF			
	$\{Zn(L_9)(HBTC)(H_2O)_2\}_n$ (**29**)				
20	$[Zn_3(L_{10})_2(dpp)_2]_n$ (**30**)	TNT	1.15×10^4	4.99×10^{-5}	83
21	$\{[Zn_2(\mu_3\text{-}OH)(cpta)(4,4'\text{-}bpy)]\cdot H_2O\}_n$ (**31**)	4-NP	4.55×10^4	4.01×10^{-6}	84
22	$[Cd(TPA)(BIB)]_n$ (**32**)	NB	1.70×10^4	2.70×10^{-7}	85
	$[Cd(TPA)(BIYB)]_n$ (**33**)	2,4-DNP	1.60×10^5	1.30×10^{-7}	
23	$\{[Zn_2(tpbn)(mbhna)_2]\cdot 4H_2O.1.5DMF\}_n$ (**34**)	4-NA	2.23×10^4	5.37×10^{-5}	86
	$\{[Cd_2(tpbn)(mbhna)_2]\cdot 2DMF\}_n$ (**35**)	4-NA	2.87×10^4	1.29×10^{-5}	
24	$\{[Cd_2(tdz)_2(4,4'\text{-}bpy)_2]\cdot 6.5H_2O\}_n$ (**36**)	TNP	4.86×10^4	6.30×10^{-6}	87
25	$[Zn(NDC)(MI)]_n$ (**37**)	TNP	4.32×10^4	5.80×10^{-6}	88
		2,6-DCNA	2.95×10^4	6.00×10^{-8}	
26	$\{[Zn_2(XN)_2(IPA)_2]\cdot 2H_2O\}_n$ (**38**)	Acetylacetone	2.30×10^3	2.49×10^{-6}	89
27	$[\{Zn(BINDI)_{0.5}(bpa)_{0.5}(H_2O)\}\cdot 4H_2O]_n$ (**39**)	TNP	4.90×10^4	2.61×10^{-6}	90
	$[\{Zn(BINDI)_{0.5}(bpe)\}\cdot 3H_2O]_n$ (**40**)	TNP	1.29×10^4	5.63×10^{-6}	
28	$[Zn_2(cptpy)(btc)(H_2O)]_n$ (**41**)	Paraquat	1.03×10^3	9.73×10^{-6}	91
29	$[Zn_2(H_2BCA)_2(o\text{-}bimb)_2(H_2O)_2]_n$ (**42**)	Acetone	3.70×10^4	9.00×10^{-8}	92
	$\{[Zn(H_2BCA)(m\text{-}bib)]\cdot H_2O\}_n$ (**43**)	Acetone	2.00×10^4	1.30×10^{-7}	
30	$\{[Zn(L_{11})_{0.5}(bimbu)]\cdot 2H_2O\cdot 0.5(CH_3)_2NH\}_n$ (**44**)	NB	3.38×10^3	8.89×10^{-6}	93
	$\{[Zn(L_{11})_{0.5}(bimb)]\cdot 4H_2O\}_n$ (**45**)	NB	2.85×10^3	1.05×10^{-5}	
	$\{[Zn(L_{11})_{0.5}(btdpe)]\cdot H_2O\}_n$ (**46**)	NB	3.75×10^3	8.00×10^{-6}	
	$[Zn(L_{11})_{0.5}(bidpe)]_n$ (**47**)	NB	4.59×10^3	6.54×10^{-6}	
31	$[Zn(opda)(bib)]_n$ (**48**)	2-NP	1.33×10^7	2.10×10^{-7}	94
31	$[Zn(ppda)(bib)(H_2O)]_n$ (**49**)	2-NP	1.42×10^7	1.86×10^{-7}	94

Table 1 *(Contd.)*

Sr no.	LCPs/LMOFs[a]	Organic analyte	K_{sv} (M^{-1})	LOD (M)	Ref.
32	$[Zn(NH_2\text{-bdc})(4,4'\text{-bipy})]_n$ (**50**)	TNP	3.10×10^4	3.20×10^{-5}	95
33	$\{Zn_2(tpt)_2(tdc)_2 \cdot H_2O\}_n$ (**51**)	TNP	7.80×10^4	2.56×10^{-6}	96
34	$[Cd_2(2\text{-abpt})(Hbtca)(H_2btca)_{0.5}(H_2O)]_n$ (**52**)	TNP	1.63×10^4	3.11×10^{-7}	97

[a] BPDC = biphenyl dicarboxylic acid; ad = adenine; ppvppa = *N*-(pyridin-2-yl)-*N*-(4-(2-(pyridin-4-yl)vinyl)phenyl)pyridin-2-amine; NDC = naphthalenedicarboxylic acid; Ur = urotropine; L_1 = 4-amino-3,5-bis(4-imidazol-1-ylphenyl)-1,2,4-triazole; 5-asba = 2-amino-5-sulfobenzoic acid; bimbu = 1,4-bis(1*H*-imidazol-1-yl)butane; L_2 = 4-pyridyl carboxaldehyde isonicotinoylhydrazone; BDC = benzene-1,4-dicarboxylic acid; BrIP = 5-bromoisophthalic acid; TIB = 1,3,5-tris(imidazol-1-ylmethyl)benzene or 1,3,5-tris(1-imidazolyl)benzene; bda = 2,2′-biphenyl dicarboxylic acid; L_3 = 5-aminoisophthalic acid; bpy = 4,4′-bipyridine; azp = 4,4′-azobipyridine; TPOM = tetrakis(4-pyridyloxy-methylene) methane; L_5 = 4,4′,4″,4‴-(1,4-phenylenebis(2-phenylethene-2,1,1-triyl))tetrabenzoic acid; L_6 = 6-(4-carboxyphenyl)-2-naphthoic acid; tpbn = *N*,*N*′,*N*″,*N*‴-tetrakis(2-pyridylmethyl)-1,4-diaminobutane; tphn = *N*,*N*′,*N*″,*N*‴-tetrakis(2-pyridylmethyl)-1,6-diaminohexane; IPA = isophthalic acid; L_7 = 3-pyridylcarboxaldehyde nicotinoylhydrazone; L_8 = 3-pyridin-3-yl-*N*-[5-(3-pyridin-3-yl-acryloylamino)-naphthalen-1-yl]-acrylamide; CHD = 1,4-cyclohexane dicaboxylic acid; PDA = 1,4-phenylenediacetic acid; Py_2TTz = 2,5-bis(4-pyridyl)thiazolo[5,4-*d*]thiazole; SDB = 4,4′-sulfonyldibenzoate; L_9 = *N*4,*N*4′-di(pyridin-4-yl) biphenyl-4,4′-dicarboxamide; BTC = 1,3,5-benzenetricarboxylic acid; L_{10} = 3,5-dibromosalicylaldehyde salicylhydrazone; dpp = 1,3-di(4-pyridyl) propane; cpta = 2-4(-carboxyphenoxy)terephthalic acid; TPA = 3,3′-thiodipropionic acid; bib = 1,4-bis(imidazol-1-yl)benzene; BIYB = 4,4-bis(imidazol-1-ylmethyl)biphenyl; mbhna = 4,4′-methylene-bis[3-hydroxy-2-naphthalene carboxylic acid; tdz = thiadiazole dicarboxylate; MI = 2-methylimidazole; XN = 4′-(4-pyridine)4,2′:2′,4″-terpyridine; BINDI = *N*,*N*′- bis(5-isophthalic acid)naphthalenediimide; bpa = 1,2-bis(4-pyridyl)ethane; bpe = 1,2-bis(4-pyridyl)ethylene; cptpy = 4-(4-carboxyphenyl)-2,2′:4′,4″-terpyridine; BCA = bis(4-carboxybenzyl)amine; bimb = 1,4-bis(imidazol-1-ylmethyl)benzene; btdpe = 4,4′-bis(4*H*-1,2,4-triazol-4-yl)diphenyl ether; bidpe = 4,4′-bis(imidazolyl)diphenyl ether; L_{11} = 5,5′-(1,4-xylylenediamino) diisophthalic acid; opda = 1,2-phenylenediacetic acid; ppda = 1,4-phenylene-diacetic acid; NH_2bdc = 2-amino-1,4-benzenedicarboxylic acid; tpt = 2,4,6-tri(pyridin-4-yl)-1,3,5-triazine; tdc = 2,5-thiophenedicarboxylic acid; abpt = 3,5-di(2-pyridyl)-4-amino-1,2,4-triazole.

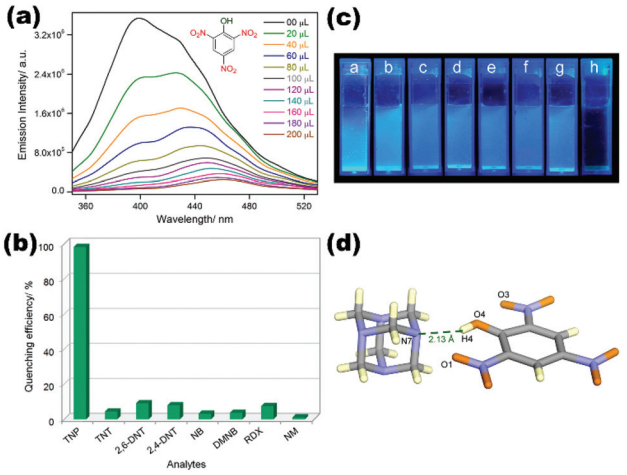

Fig. 1 (a and b) Emission spectra of (**3**) dispersed in water, upon incremental addition of aqueous TNP solution (1 mM) and quenching efficiency plot for different NACs; (c) response of (**3**) aqueous dispersions toward the additions of various NAC solutions under UV light (λ_{max} = 365 nm) (*a* = TNT, *b* = NM, *c* = RDX, *d* = 2,4-DNT, *e* = 2,6-DNT, *f* = NB, *g* = DMNB, *h* = TNP); (d) crystal structure of the co-crystal **1** Ur-TNP revealing intermolecular H-bonding interactions. Reproduced with permission from ref. 66. Copyright 2015 American Chemical Society.

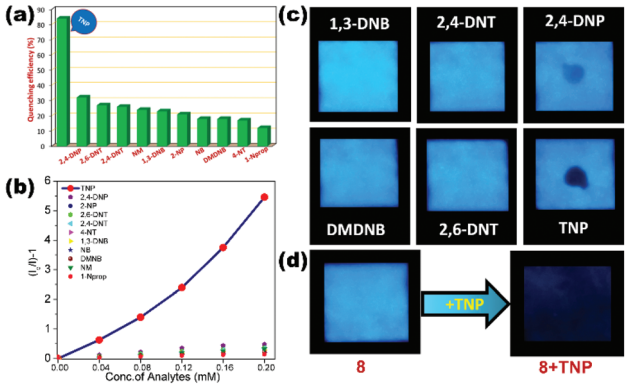

Fig. 2 (a) Quenching efficiency of (**8**) for different nitro analytes; (b) Stern–Volmer traces of various nitro analytes (0–200 μL; 2 mM) in a water suspension of (**8**) (2 mg/2 mL); (c) digital photographs of paper strips coated with (**8**) after adding various nitro analytes under UV light (365 nm); (d) the paper strip dipped in 2 mM aqueous solution of TNP for 10 s showed full darkening of paper strip of (**8**). Reproduced with permission from ref. 70. Copyright 2016 Royal Society of Chemistry.

of L_2 and the hydroxyl group of TNP *via* co-crystal formation.[69] In another example, two dimensional Cd(II) MOFs $[Cd(5\text{-BrIP})(TIB)]_n$ (**8**) synthesized by our group using tripodal N-donor 1,3,5-tris(imidazol-1-ylmethyl)benzene (TIB) and 5-bromoisophthalate (5-BrIP) showed excellent photoluminescence properties in the solid state and in water. Fluorescence properties of the chemically stable (**8**) are exploited for the selective detection of TNP from a large pool of other nitroaromatics. Excellent sensing behaviour of (**8**) for TNP is visible from K_{sv} and LOD values (2.68×10^4 M^{-1} and 2.70×10^{-5} M). LMOF (**8**) coated on the paper strip demonstrates a fast response of TNP for the practical application of explosive detection (Fig. 2).

Electrostatic interaction between TNP and TIB linkers as well as the energy transfer phenomenon favours the quenching mechanism.[70] Similarly, the tripodal TIB ligand based water stable MOF $\{[Cd_2(tib)_2(bda)_2]\cdot G\}_n$ (**9**) synthesized by Bu *et al.* demonstrated excellent acetone sensing *via* fluorescence quenching. The crystal structure of LMOF (**9**) exposed a double helical motif generated *via* 2,2′-biphenyl dicarboxylate (bda) coordination, which enhances the water stability. The aqueous

solution of acetone (0.7 vol%) completely quenched the emission intensity of (**9**) amid other organic solvent molecules.[71]

Neogi *et al.* hydrothermally synthesized two luminescent MOFs $\{[Zn_2(L_3)_2(bpy)]\cdot(DMF)\cdot(H_2O)_2\}_n$ (**10**) and $\{[Zn_2(L_3)_2(azp)]\cdot(DMF)_2\cdot(H_2O)\}_n$ (**11**) comprising 5-aminoisophthalate (L_3) and N-donor pillar bpy/azp. Both pillar-layer LMOFs showed high chemical stability in water and possess good luminescence behaviour in the aqueous phase. They utilized both (**10**) and (**11**) for the selective and sensitive detection of high explosive TNP molecules with K_{sv} values 1.53×10^4 M^{-1} and 3.11×10^4 M^{-1} and lower detection limit values 3.48×10^{-6} M and 1.82×10^{-6} M respectively compared to other NACs. The detection mechanism revealed both static and dynamic quenching behaviour with a resonance energy transfer (RET) phenomenon. Strong non-covalent interactions observed in the co-crystal of TNP and N-donor azp also correlated to support the quenching mechanism.[72] Highly fluorescent $\{Zn_2(H_2L_5)_2(bpy)_2(H_2O)_3\cdot H_2O\}_n$ (**12**) constructed from an active tetraphenylene derivative L_5 (4,4′,4″,4‴-(1,4-phenylenebis(2-phenylethene-2,1,1-triyl))tetrabenzoic acid) and bpy as a result of aggregation-induced emission (AIE) is reported by Zhao and co-workers. LMOF (**12**) showed good water stability and high quantum yield (43%) which is successfully applied for the chemical sensing of the TNP molecule showing quenching constant 1.36×10^4 M^{-1} and detection limit 4.9×10^{-5} M. The electron-donating nature of (**12**) is effective for the detection of electron-deficient nitro explosives with good sensitivity. The electron transfer process which is enlightened by photo-induced electron transfer (PET) and also fluorescence resonance energy transfer (FRET) reinforced by the non-linear Stern–Volmer plot for the quenching process is advocated.[73] Luminescent neutral Zn(II) coordination polymer $[Zn(\mu_2\text{-1Had})(\mu_2\text{-}SO_4)]_n$ (**13**) synthesized from biomolecule adenine (ad) reported by our group possesses excellent fluorescence properties in solid-state as well as in water suspension. The luminescence behaviour of (**13**) is successfully exploited for the ultrasensitive detection of TNP with K_{sv} 3.14×10^4 M^{-1} and a remarkable LOD value of 4.00×10^{-10} M.

The quenching mechanism is explained by strong electrostatic interaction between the free nitrogen atoms of adenine and TNP molecule which is responsible for electron/energy transfer processes. A possible hydrogen bonding interaction between the amino group of the adenine linker and the acidic TNP analyte also plays important roles in high sensitivity. An LCP (**13**) coated paper strip also has been developed for the visible detection of nitro derivatives which shows the quenching effect under irradiated UV light suggesting the practical applicability of these materials (Fig. 3).[74] Bharadwaj *et al.* reported the synthesis and fluorescence sensing ability of porous 2D coordination polymer $\{[Zn_3(L_6)_3(Ur)_2]\cdot 2DMF\cdot 3H_2O\}_n$ (**14**) constructed from the naphthalene based linker L_6 (6-(4-carboxyphenyl)-2-naphthoic acid) and urotropine (Ur). Fluorescent naphthalene ligand dependent excellent emission displayed by LCP (**14**) is efficient to recognise the TNP explosive in the aqueous phase with quenching constant 5.10×10^4 M^{-1} and detection limit 8.46×10^{-6} M.[75]

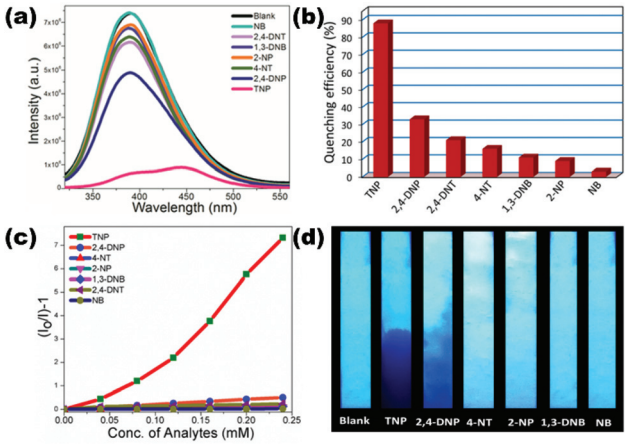

Fig. 3 (a) Emission spectra of aqueous dispersed (**13**) after addition of aqueous solutions of NACs; (b) emission quenching (%) of (**13**) upon addition of different NACs; (c) Stern–Volmer plots for (**13**) upon gradual addition of NACs; (d) digital images of (**13**)-coated test strips after they were dipped in aqueous solutions of NACs. Reproduced with permission from ref. 74. Copyright 2017 American Chemical Society.

Similarly, Mandal and co-workers demonstrated the TNP sensing ability of mixed ligand 2D LMOFs namely $\{Zn_2(tpbn)(2,6\text{-}NDC)_2\}_n$ (**15**) and $\{[Zn_2(tphn)(2,6\text{-}NDC)_2]\cdot 4H_2O\}_n$ (**16**). Both mixed ligand LMOFs comprise naphthalene dicarboxylate and pyridine-based N-donor linkers tpbn (*N*,*N*′,*N*″,*N*‴-tetrakis(2-pyridylmethyl)-1,4-diaminobutane)/tphn (*N*,*N*′,*N*″,*N*‴-tetrakis(2-pyridylmethyl)-1,6-diaminohexane). The selective and sensitive sensing of TNP with Stern–Volmer constant and LOD values by (**15**) and (**16**) were 5.90×10^3 M^{-1}, 2.46×10^3 M^{-1} and 4.75×10^{-5} M, 8.11×10^{-5} M respectively.[76] Mechanochemically synthesized isostructural 2D dual ligand coordination polymers $\{[Zn(IPA)(L_7)]\}_n$ (**17**) and $\{[Cd(IPA)(L_7)]\}_n$ (**18**) comprising isophthalate (IPA) and Schiff base N-donor pillar L_7 (3-pyridylcarboxaldehyde nicotinoylhydrazone) reported by our group displayed excellent water stability and luminescence properties in the aqueous phase. Both LCPs selectively detect the TNP molecule with high quenching constant values of 2.16×10^4 M^{-1} (**17**) and 1.52×10^4 M^{-1} (**18**) among other nitroanalytes. The sensitivity of both LCPs for TNP was demonstrated by excellent limit of detection values of 1.20×10^{-7} M (**17**) and 6.00×10^{-8} M (**18**). For understanding of the sensing mechanism, spectral overlap between the UV absorption of NACs and emission of LCPs displaying a clear overlap for TNP suggesting energy transfer processes is responsible for fluorescence quenching. Fluorescence microscopy images captured under a visible/UV filter for pristine LCPs and TNP added LCPs displayed complete quenching of the emission intensity (Fig. 4).[77]

A mixed ligand luminescent Zn(II) based 3D MOF $\{Zn_4(TPOM)(1,4\text{-}NDC)_4\}_n$ (**19**) constructed from tetrapodal semi-rigid N-donor linker TPOM (tetrakis(4-pyridyloxy-methylene)methane) and 1,4-naphthalene dicarboxylate (NDC) has been reported by Mandal and co-workers for amine sensing ability. MOF (**19**) with good chemical stability and recyclability

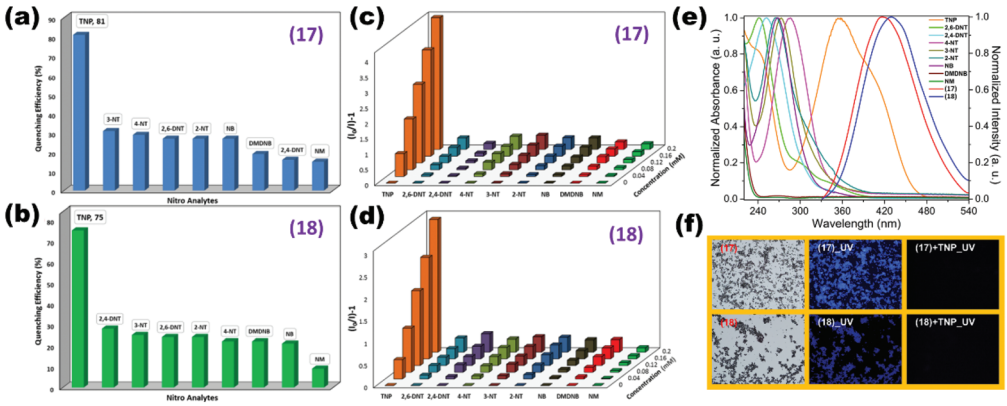

Fig. 4 (a and b) Quenching (%) of aqueous suspensions of (**17**) and (**18**) for different NACs. (c and d) Stern–Volmer (SV) plots for various NACs in aqueous suspensions of (**17**) and (**18**); (e) spectral overlap between aqueous phase UV spectra of NACs and fluorescence spectra of (**17**) and (**18**); (f) microscopy images under a white light/UV filter for both CPs and under a UV filter after the addition of TNP. Reproduced with permission from ref. 77. Copyright 2017 American Chemical Society.

in aqueous medium revealed excellent sensing ability towards nitro aniline derivatives 4-NA and 2,6-DCNA (pesticide) with K_{sv} values of 7.87×10^4 M^{-1} and 2.74×10^4 M^{-1} and LOD values of 6.40×10^{-7} M and 1.39×10^{-6} M respectively.[78] In a recent report, four mixed ligand luminescent coordination polymers containing a Cd(II)/Zn(II) metal node, naphthalene core based acylamide functionalized N-donor linker L_8 (3-pyridin-3-yl-*N*-[5-(3-pyridin-3-yl-acryloylamino)-naphthalen-1-yl]-acrylamide and different carboxylate derivatives have been unveiled. All LCPs $[Cd(L_8)(IPA)]_n$ (**20**), $\{[Zn_2(L_8)(L_3)_2]\cdot 3H_2O\}_n$ (**21**), $\{Cd(L_8)(PDA)(H_2O)_2\}_n$ (**22**) and $\{[Cd_3(L_8)(CHD)_3(DMF)_2]\cdot 2DMF\}_n$ (**23**) have been successfully utilized for the aqueous phase detection of nitrophenol derivative 4-NP with very good quenching constants 1.86×10^4 M^{-1}, 2.93×10^4 M^{-1}, 1.89×10^4 M^{-1} and 3.11×10^4 M^{-1} respectively. LCP (**21**) showed good sensing ability towards TNP also with a quenching constant of 4.19×10^4 M^{-1} with a detection limit of 6.90×10^{-5} M. Non-linear Stern–Volmer behaviour suggests static and dynamic quenching and spectral overlap between the emission fluorophore and analyte absorption band supporting the resonance energy transfer (RET) quenching mechanism in operation.[79] Doubly interpenetrated 3D fluorescent Zn(II)/Cd(II) MOFs $\{[Zn_2(Py_2TTz)_2(BDC)_2]\cdot 2(DMF)\cdot 0.5(H_2O)\}_n$ (**24**) and $\{[Cd_2(Py_2TTz)_2(BDC)_2]\cdot 2(DMF)\}_n$ (**25**) assembled using thiazole based pyridyl linker Py_2TTz (2,5-bis(4-pyridyl)thiazolo[5,4-*d*]thiazole) and benzene dicarboxylate (BDC) reported by Zang and co-workers were revealed as potential fluorosensors for TNP and antibiotic NZF.

Crystallographic analysis revealed that both LMOFs possess three dimensional nets with 2-fold interpenetration and *pcu* topology. Good fluorescence properties of (**24**) and (**25**) in the aqueous phase selectively detect trace amounts of explosive molecule TNP with LOD values 9.30×10^{-5} M and 9.00×10^{-5} M as well as antibiotic NZF with LOD values 9.10×10^{-5} M and 8.50×10^{-5} M respectively. Excellent K_{sv} values for TNP 3.25×10^4 M^{-1} (**24**) and 4.06×10^4 M^{-1} (**25**) and for NZF 1.72×10^4 M^{-1} (**24**) and 4.53×10^4 M^{-1} (**25**) demonstrate the selectivity among other NACs/antibiotics. The sensing mechanism is corroborated with density functional theory (DFT) calculations *via* HOMO–LUMO energy differences and is also supported by life time decay profiles for static–dynamic quenching and spectral overlap experiments for energy transfer processes (Fig. 5).[80] Cd(II) based luminescent dual ligand 3D MOF $\{[Cd_3(SDB)_3(TIB)](H_2O)_2(1,4\text{-dioxane})(G)_x\}_n$ (**26**) hydrothermally synthesized using angular dicarboxylate (SDB) and flexible imidazole containing an N-donor linker and the sensing application have been reported by us recently. LMOF (**26**) has been proved to be an excellent material for the selective adsorption and detection of the nitroaromatic pollutant TNP. The aqueous solution of TNP completely quenches the fluorescence intensity of **26** and exhibits non-linear Stern–Volmer

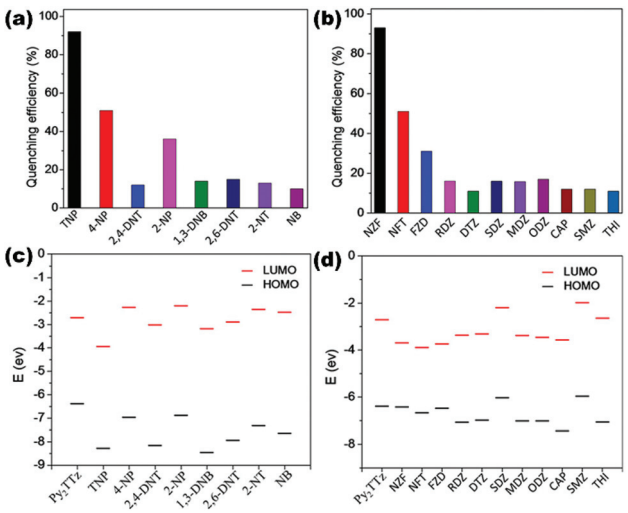

Fig. 5 (a and b) Quenching (%) for (**24**) upon addition of different NACs and antibiotics; (c and d) Comparisons of HOMO and LUMO energies for linker Py2TTz with selected NACs and antibiotics. Reproduced with permission from ref. 80. Copyright 2018 American Chemical Society.

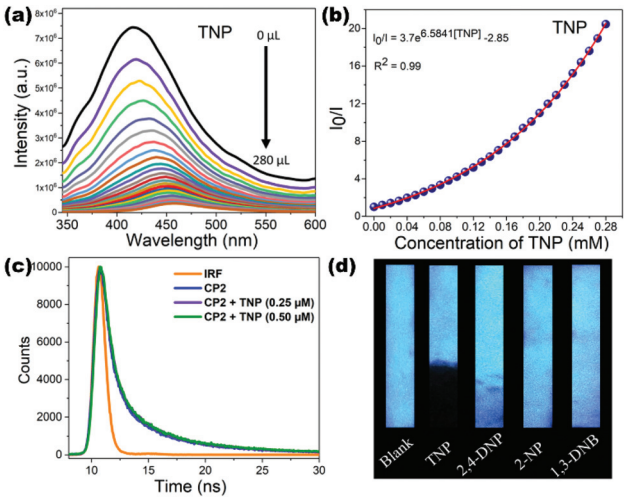

Fig. 6 (a) Fluorescence titration experiment for (**26**) upon gradual addition of TNP solution in water; (b) Stern–Volmer plot for (**26**) upon incremental addition of aqueous solution of TNP; (c) lifetime decay profiles of (**26**) in the presence and absence of TNP solution in water; (d) digital photograph of (**26**)-coated paper strips after being dipped in aqueous solutions of NACs. Reproduced with permission from ref. 81. Copyright 2018 American Chemical Society.

behaviour with K_{sv} value 2.43×10^4 M^{-1}. Static as well as dynamic quenching behaviour was evaluated by lifetime decay experiments before and after the addition of TNP to the aqueous suspension of (**26**) which showed no change in florescence lifetime supporting the non-linear SV plots. High sensitivity of (**26**) towards the detection of TNP is evident from the good limit of detection value of 1.50×10^{-5} M compared to other NACs. This fact is further supported by the visually observable cessation of fluorescence emission of the (**26**)-coated paper stripes in presence of TNP as shown in Fig. 6.[81]

Li *et al.* employed a series of newly synthesized Zn-MOFs to be scanned as potential explosive/antibiotic sensors by combining ligands based on the amide functionalized linker L_9 (*N*4,*N*4′-di(pyridin-4-yl)biphenyl-4,4′-dicarboxamide) in combination with different carboxylates. Thus, three luminescent MOFs $\{Zn(L_9)(L_3)(H_2O)\}_n$ (**27**), $\{Zn(L_9)(IPA)(DMF)(H_2O)_{1.5}\}_n$ (**28**) and $\{Zn(L_9)(HBTC)(H_2O)_2\}_n$ (**29**) for the aqueous phase detection of TNP from various other nitroaromatics and NZF among other antibiotics have been deliberated *via* a fluorescence quenching phenomenon.[82] All of the aforementioned MOFs showed pronounced fluorescence quenching upon interaction with TNP and NZF compounds compared to other NACs/antibiotics. One of the rare reports by Wu *et al.* demonstrates aqueous phase TNT sensing by a dual ligand Zn(II) coordination polymer $[Zn_3(L_{10})_2(dpp)_2]_n$ (**30**) constructed by an acyl amide linker L_{10} (3,5-dibromosalicylaldehyde salicylhydrazone). LCP (**30**) detects the highly explosive TNT with good sensitivity (K_{sv} value 1.15×10^4 M^{-1} and LOD value 4.99×10^{-5} M respectively).[83] Three dimensional LMOF $\{[Zn_2(\mu_3\text{-OH})(cpta)(4,4'\text{-bpy})]\cdot H_2O\}_n$ (**31**) synthesized using a V-shaped semi-rigid linker cpta (2-4(-carboxyphenoxy)terephthalic acid) in conjunction with N-donor (4,4′-bpy) reported by Wang and co-workers has exhibited excellent sensing ability towards nitrophenol derivative 4-NP with K_{sv} 4.55×10^4 M^{-1} and LOD value 4.01×10^{-6} M in water.[84] Fu *et al.* provided an in depth spectroscopic study of the fluorescence quenching mechanisms of two new Cd(II) based dual linker fluorescent coordination polymers $[Cd(TPA)(BIB)]_n$ (**32**) and $[Cd(TPA)(BIYB)]_n$ (**33**) for the aqueous detection of nitrobenzene (K_{sv} = 1.70×10^4 M^{-1}; LOD = 2.70×10^{-7} M) and 2,4-DNP (K_{sv} = 1.60×10^5 M^{-1}; LOD = 1.30×10^{-7} M).[85]

Two dual ligand luminescent MOFs $\{[Zn_2(tpbn)(mbhna)_2]\cdot 4H_2O.1.5DMF\}_n$ (**34**) and $\{[Cd_2(tpbn)(mbhna)_2]\cdot 2DMF\}_n$ (**35**) comprising naphthalene/hydroxyl functionalized dicarboxylate mbhna (4,4′-methylene-bis[3-hydroxy-2-naphthalene carboxylic acid) along with an N-donor ligand showed amine sensing ability especially 4-NA with K_{sv} values 2.23×10^4 M^{-1}, 2.87×10^4 M^{-1} and LOD values 5.37×10^{-5} M, 1.29×10^{-5} M respectively. The sensing mechanism is elucidated by spectral overlap and HOMO–LUMO energy calculations.[86] Three dimensional MOF $\{[Cd_2(tdz)_2(4,4'\text{-bpy})_2]\cdot 6.5H_2O\}_n$ (**36**) constructed from flexible thiadiazole dicarboxylate (tdz) and bpy exhibits excellent luminescence properties in the aqueous phase. The high chemical stability of LMOF (**36**) is utilized for TNP detection showing good quenching constant 4.86×10^4 M^{-1} and detection limit 6.30×10^{-6} M amid other nitroaromatics.[87] Zn(II) based fluorescent 2D coordination polymer $[Zn(NDC)(MI)]_n$ (**37**) synthesized using mixed linker naphthalene dicarboxylate and 2-methylimidazole displayed excellent stability and emission properties in water. The aqueous phase suspension of LCP (**37**) attested selective and recyclable detection of explosive molecule TNP and pesticide 2,6-DCNA with exceptional SV constant values 4.32×10^4 M^{-1} and 2.95×10^4 M^{-1} respectively. The sensitivity of (**37**) towards pollutant recognition is well supported by lower detection values 5.80×10^{-6} M (TNP) and 6.00×10^{-8} M (2,6-DCNA). The fluorescence quenching phenomenon is explained on the basis of simultaneous effects of PET and FRET processes (Fig. 7).[88]

Selective and sensitive sensing of the acetylacetone solvent molecule was achieved using a thermally and chemically stable luminescent Zn(II) MOF $\{[Zn_2(XN)_2(IPA)_2]\cdot 2H_2O\}_n$ (**38**) with a good K_{sv} value of 2.30×10^3 M^{-1} and an LOD value of 2.49×10^{-6} M.[89] Nagaraja *et al.* reported the solvothermal synthesis of a Zn^{2+} MOF with the formula $[\{Zn(BINDI)_{0.5}(bpa)_{0.5}(H_2O)\}\cdot 4H_2O]_n$ (**39**) and $[\{Zn(BINDI)_{0.5}(bpe)\}\cdot 3H_2O]_n$ (**40**) constructed from electron rich dicarboxylate BINDI (*N*,*N*′-bis(5-isophthalic acid)naphthalenediimide) and N-donor ligands and their luminescence properties. Water stability and aqueous phase fluorescence properties of both LMOFs have been exploited for the selective and sensitive sensing of TNP with excellent K_{sv} and limit of detection values (K_{sv} 4.90×10^4 M^{-1} (**39**), 1.29×10^4 M^{-1} (**40**); LOD 2.61×10^{-6} M (**39**), 5.63×10^{-6} M (**40**)).[90] 3D LMOF $[Zn_2(cptpy)(btc)(H_2O)]_n$ (**41**) was hydrothermally synthesized by the combination of terpyridine based N-donor cptpy (4-(4-carboxyphenyl)-2,2′:4′,4″-terpyridine) and benzene tricarboxylate exhibiting excellent luminescence sensing behaviour towards herbicide molecule paraquat (PAQ). The sensing ability of (**41**) for PAQ by a

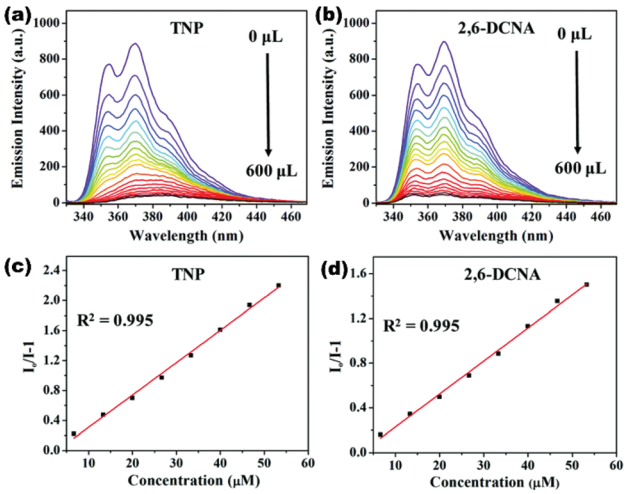

Fig. 7 (a and b) Reduction in emission intensity of (**37**) dispersed in water after incremental addition of TNP and 2,6-DCNA; (c and d) the Stern–Volmer plot of (**37**) for TNP and 2,6-DCNA. Reproduced with permission from ref. 88. Copyright 2019 Royal Society of Chemistry.

Stern–Volmer constant was 1.03×10^3 M^{-1} with a lower detection value of 9.73×10^{-6} M.[91] Secondary amine based flexible dicarboxylate bis(4-carboxybenzyl)amine (BCA) containing 3D LCPs $[Zn_2(H_2BCA)_2(o\text{-}bimb)_2(H_2O)_2]_n$ (**42**) and $\{[Zn(H_2BCA)(m\text{-}bib)]\cdot H_2O\}_n$ (**43**) has shown excellent sensory material properties towards acetone in water. The quenching constant values 3.70×10^4 M^{-1} (**42**), 2.00×10^4 M^{-1} (**43**) and limit of detection values 9.00×10^{-8} M (**42**), 1.30×10^{-7} M (**43**) clearly demonstrated the potential of both LCPs for aqueous phase acetone detection.[92]

Fan and co-workers described the potential of dual ligand diisophthalate based LMOFs $\{[Zn(L_{11})_{0.5}(bimbu)]\cdot 2H_2O\cdot 0.5(CH_3)_2NH\}_n$ (**44**), $\{[Zn(L_{11})_{0.5}(bimb)]\cdot 4H_2O\}_n$ (**45**), $\{[Zn(L_{11})_{0.5}(btdpe)]\cdot H_2O\}_n$ (**46**) and $[Zn(L_{11})_{0.5}(bidpe)]_n$ (**47**) for selective nitrobenzene (NB) sensing. All LMOFs showed very good K_{sv} values in the range of $2.85–4.59 \times 10^3$ M^{-1} and LOD values in the range of $0.10–8.89 \times 10^{-6}$ M for NB detection in water.[93] Two 3D dual linker LCPs $[Zn(opda)(bib)]_n$ (**48**) and $[Zn(ppda)(bib)(H_2O)]_n$ (**49**) displayed selective sensing of nitrophenol derivative 2-NP in aqueous media. Both LCPs showed outstanding K_{sv} values 1.33×10^7 M^{-1} (**48**), 1.42×10^7 M^{-1} (**49**) and excellent LOD values 2.10×10^{-7} M (**48**), 1.86×10^{-7} M (**49**) for 2-NP recognition.[94] Amino functionalized Zn(II) LMOF $[Zn(NH_2\text{-}bdc)(4,4'\text{-}bipy)]_n$ (**50**) demonstrated unique sensing behaviour towards the TNP molecule *via* fluorescence turn on (ethanol) and turn off (water). The aqueous phase detection ability of (**50**) for TNP was established by a quenching constant (K_{sv}) value of 3.10×10^4 M^{-1} and LOD value 3.20×10^{-5} M.[95] Of late, Zhang *et al.* reported mixed ligand LCP $\{Zn_2(tpt)_2(tdc)_2\cdot H_2O\}_n$ (**51**) for sensitive sensing of TNP in water with an ultra-high quenching constant value of 7.80×10^4 M^{-1} and a detection value of 2.56×10^{-6} M.[96] Similarly, dual linker Cd(II) LMOF $[Cd_2(2\text{-}abpt)(Hbtca)(H_2btca)_{0.5}(H_2O)]_n$ (**52**) was synthesized from triazole containing abpt (3,5-di(2-pyridyl)-4-amino-1,2,4-triazole) employed as a fluorosensor for TNP in water with very good quenching constant of 1.63×10^4 M^{-1} and detection limit of 3.11×10^{-7} M.[97] The aqueous phase sensing and detection of organic pollutants such as solvents and precursors used for the synthesis of value-added chemicals and nitro organic compounds which are not only industrially important molecules but also hazardous and explosive in nature is synchronised in this inclusive review using a Zn(II)/Cd(II) based fluorosensor.

Inorganic pollutants

The importance of inorganic ionic species in different areas of chemistry such as biology, medicine, catalysis and environment has triggered the momentum for their selective recognition and sensing in recent years. Anions and cations play a significant role in different capacities in chemical, biological and environmental processes, establishing their importance and are widely distributed in nature and organisms.[98,99] During the industrial production of value-added chemicals and as a catalyst, molecules with inorganic components are extensively used and some of these hazardous untreated inorganic species released to soil and aquatic bodies can cause environmental pollution. Due to the wide-ranging utilization as a strong oxidant, metal derived oxoanions such as $Cr_2O_7^{2-}$, CrO_4^{2-}, MnO_4^-, *etc.* which are noxious inorganic pollutants have been extensively used in various industrial processes. For example, $Cr_2O_7^{2-}$ has been widely used in industrial processes, including electroplating, paint manufacturing, tanning, and steel fabrication *etc.*, and the improper disposal of industrial waste containing chromium can contaminate soil and water sources harming the environment. A trace amount of highly toxic carcinogenic Cr(VI) can induce DNA damage and allergic reactions such as ulcers, renal failure, lung cancer, *etc.* eventually causing a high threat to human health.[100–102] A requisite amount of Fe^{3+} ions plays an important role in the physiological and biochemical processes of the human body and the deficiency can cause serious diseases such as anaemia or excess can induce damage to liver and kidneys.[103,104] As is well known, Hg^{2+} and Pb^{2+} are harmful and dangerous inorganic pollutants, which are difficult to degrade and having a bioaccumulative effect on the ecosystem causing environmental issues and human health. It has been documented in the literature that the accumulation of Hg^{2+} and Pb^{2+} through food chains can cause serious damage to central nervous and immune systems, protein synthesis and so on.[105] On the other hand, the risk of aluminum contamination is threatening to human health considering its usage and distribution causing toxicity to human health and can induce diseases such as softening of the bones, osteoporosis, rickets, *etc.* including Alzheimer's disease.[106,107] The mentioned concerns which have relevance in environmental protection and human health have driven research efforts to develop new materials as chemical sensors for detecting the minute concentrations of toxic ions in soils and water bodies. Luminescent coordination polymers (LCPs) and luminescent metal organic frameworks (LMOFs) have emerged as excellent chemical sensors for the detection of pollutants or analytes causing threat to environ-

ment/human health and the present section deals with a comprehensive review of sensing and detection of inorganic pollutants in the aqueous phase since 2015. The classification of inorganic pollutants mainly includes different hazardous metal cations such as Hg^{2+}, Fe^{3+}, Pb^{2+}, Pd^{2+}, Cr^{3+}, Al^{3+}, Cu^{2+} and anionic species *viz.* CrO_4^{2-}, $Cr_2O_7^{2-}$, MnO_4^-, CN^-, I^-. Aqueous phase detection by Zn(II)/Cd(II) mixed ligand LMOFs of the mentioned pollutants has been summarised in Table 2 and abridged in this section.

Highly luminescent mixed ligand Cd(II)-MOFs $[Cd_3(L_{12})(bipy)_2(DMA)_4]_n$ (**53**), $[Cd_6(L_{12})_2(bibp)_2(DMA)_4]_n$ (**54**) and $[Cd_3(L_{12})(tib)(DMF)_2]_n$ (**55**) consisting of a semi rigid linker L_{12} (hexa[4-(carboxyphenyl)oxamethyl]-3-oxapentane acid) in combination with different N-donor spacers has been synthesized using the solvothermal method by Sun *et al.* All three LMOFs possess a 3D structure and are utilized for the selective detection of chromate anions among other interfering anions *via* fluorescence quenching. Chromate anions completely quenched the luminescence intensity of LMOFs in the aqueous phase which is explained by the weak interaction of analytes with frameworks and energy adsorption competition between analytes/LMOFs.[108] On the other hand, the Zn(II) coordination polymer $[Zn_2(L_{13})_2(bpe)_2(H_2O)_2]_n$ (**56**) reported by Lang *et al.* comprising flexible dicarboxylate L_{13} (4,4′-((1,2-phenylenebis(methylene))bis(oxy))dibenzoic acid) and N-donor linker bpe ((E)-1,2-di(pyridin-4-yl)ethene) is known for exclusive sensing of the Fe^{3+} cation. The fluorescence intensity of LCP (**56**) was quenched by Fe^{3+} in aqueous solution with K_{sv} value 2.39×10^3 M^{-1} and a limit of detection value 2.50×10^{-5} M.[109] Wen *et al.* reported two amino decorated luminescent dual ligand MOFs $[Zn(2\text{-}NH_2bdc)(bibp)]_n$ (**57**) and $[Cd(2\text{-}NH_2bdc)(tib)(H_2O)_4(DMA)_{0.5}]_n$ (**58**) constructed from 2-aminotherephthalate (2-NH_2bdc) and imidazole based N-donor spacers. LMOF (**57**) is applicable as an excellent bifunctional fluorosensor for selective and sensitive detection of the Hg^{2+} cation and $Cr_2O_7^{2-}$ anion *via* a quenching phenomenon (Fig. 8). The selectivity and sensitivity of **57** towards respective analytes is validated by high K_{sv} values 4.55×10^3 M^{-1} (for Hg^{2+}) and 6.55×10^6 M^{-1} (for $Cr_2O_7^{2-}$). Similarly, LMOF (**58**) is also an excellent fluorosensor for Hg^{2+} with a limit of detection value 4.20×10^{-8} M in the aqueous phase.[110]

Doubly interpenetrated 3D mixed linker MOF $[Zn_5(hfipbb)_4(trz)_2(H_2O)_2]_n$ (**59**) synthesized from V-shaped dicarboxylate (hfipbb = 4,4-(hexafluoroisopropylidene)bis(benzoic acid)) and triazole ligands exhibited excellent luminescence properties and chemical stability in water due to the presence of a hydrophobic CF_3 functional group. The luminescence properties of (**59**) have been successfully utilized for the fluorescence sensing of Fe^{3+} in water with LOD value 2.00×10^{-4} M. The quenching effect underlined by overlapping of the absorption spectrum of Fe^{3+} with the emission spectrum of LMOF (**59**) suggests the competition for excitation energy between the analyte and host resulting in a decrease of emission intensity.[111]

As discussed earlier, LMOF (**5**) was also utilized as a luminescent sensor for inorganic pollutant cation Fe^{3+} with quenching constant 1.78×10^4 M^{-1} and detection limit 1.87×10^{-4} M in water as well as in HEPES buffer solution for simulative physiological conditions towards biological application.[68] In another report, Wen and co-workers constructed two mixed linker luminescent MOFs $[Zn(L_4)(BBI)\cdot(H_2O)_2]_n$ (**60**) and $[Cd(L_4)(TPOM)_{0.75}]\cdot xG$ (**61**) using thiophene based carboxylate (L_4 = (benzo-(1,2;4,5)-bis(thiophene-2′-carboxylic acid) and N-donor ligands (BBI = 1,1′-(1,4-butanediyl)bis(imidazole), TPOM = tetrakis(4-pyridyloxy-methylene)methane). Both LMOFs showed excellent photoluminescence properties in the aqueous phase and was exposed as a competent sensory material for inorganic cations/anions (Cu^{2+}, Hg^{2+}, $Cr_2O_7^{2-}$). LMOF (**60**) selectively detected the contaminates Hg^{2+} and $Cr_2O_7^{2-}$ with K_{sv} values 9.39×10^3 M^{-1} and 1.16×10^4 M^{-1} respectively. Similarly, LMOF (**61**) showed excellent sensing ability for Cu^{2+} and $Cr_2O_7^{2-}$ with quenching constant values 1.78×10^4 M^{-1} and 1.34×10^4 M^{-1} respectively. The diffusion of guest metal ions into the pores of LMOFs and non-covalent interaction of analyte/LMOFs paves the way for the energy transfer mechanism for the quenching phenomenon.[112] Ghosh *et al.* demonstrated a chemodosimetric approach for the recognition of a highly toxic cyanide (CN^-) anion using a cationic dye incorporated MOF $[Zn_8(ad)_4(BPDC)_6O.2Me_2NH_2]\cdot G$@DAAC (**62**). In the MOF (**62**) guest solvent molecules were replaced by a cationic dye molecule (3,6-diaminoacridinium cation (DAAC)) which is selectively reacted with cyanide anion turning on the fluorescence properties of MOF. A superb sensing ability of (**62**) supported by a limit of detection value of 1.93×10^{-8} M as well as biocompatibility of the MOF is useful for *in vitro* sensing of the cyanide anion in aqueous media.[113] Previously discussed LCP $[Zn(\mu_2\text{-}1Had)(\mu_2\text{-}SO_4)]_n$ (**13**) also showed an admirable fluorescence quenching response towards highly toxic metal cation mercury (Hg^{2+}) in water with quenching constant 7.7×10^3 M^{-1} amid other interfering cations. The sensitivity of **13** is demonstrated by excellent detection limit 7.00×10^{-8} M for mercury which is further sustained by LCP coated test paper strip detection (Fig. 9). The quenching mechanism is enlightened by a probable interaction of the Hg^{2+} cation with free heterocyclic nitrogen and amino functionality on an adenine ligand.[74]

Zn(II) based 2D luminescent MOF $\{[Zn(2,5\text{-}tdc)(3\text{-}abit)]\cdot H_2O\}_n$ (**63**) synthesized by a combination of ligands namely 2,5-thiophenedicarboxylic acid (2,5-tdc) and 4-amino-3,5-bis(imidazol-1-ylmethyl)-1,2,4-triazole (3-abit) showed good water stability and selective sensing properties for inorganic anions (CrO_4^{2-}; $Cr_2O_7^{2-}$) in water. The corresponding detection ability was determined by quenching constant values 5.43×10^3 M^{-1} (CrO_4^{2-}) and 5.08×10^3 M^{-1} ($Cr_2O_7^{2-}$).[114] Zheng *et al.* explored two mixed linker Cd(II) based LMOFs $\{[Cd(L_{14})(BPDC)]\cdot 2H_2O\}_n$ (**64**) and $\{[Cd(L_{14})(SDBA)(H_2O)]\cdot 0.5H_2O\}_n$ (**65**) constructed using N-donor linker L_{14} (4,4′-(2,5-bis-(methylthio)-1,4-phenylene)dipyridine) and dicarboxylates SDBA/BPDC. Both LMOFs were productively employed as selective fluorosensors for chromate anions and Fe^{3+} cations in the aqueous phase. Sensing ability for $Cr_2O_7^{2-}$ was well explored by Stern–Volmer con-

Table 2 List of Zn(II)/Cd(II) mixed ligand LCP/LMOF sensors for aqueous-phase detection of inorganic pollutants

Sr no.	LMOFs/LCPs[a]	Inorganic analyte	K_{sv} (M^{-1})	LOD (M)	Ref.
1	$[Cd_3(L_{12})(bipy)_2(DMA)_4]_n$ (**53**)	CrO_4^{2-}	—	—	108
	$[Cd_6(L_{12})_2(bibp)_2(DMA)_4]_n$ (**54**)	$Cr_2O_7^{2-}$			
	$[Cd_3(L_{12})(tib)(DMF)_2]_n$ (**55**)				
2	$[Zn_2(L_{13})_2(bpe)_2(H_2O)_2]_n$ (**56**)	Fe^{3+}	2.39×10^3	2.50×10^{-5}	109
3	$[Zn(2\text{-}NH_2bdc)(bibp)]_n$ (**57**)	Hg^{2+}	4.55×10^3	—	110
		$Cr_2O_7^{2-}$	6.55×10^6		
	$[Cd(2\text{-}NH_2bdc)(tib)(H_2O)_4(DMA)_{0.5}]_n$ (**58**)	Hg^{2+}	—	4.20×10^{-8}	
4	$[Zn_5(hfipbb)_4(trz)_2(H_2O)_2]_n$ (**59**)	Fe^{3+}	—	2.00×10^{-4}	111
5	$\{[Cd(5\text{-}asba)(bimbu)]\}_n$ (**5**)	Fe^{3+}	1.78×10^4	1.87×10^{-4}	68
6	$[Zn(L_4)(BBI)\cdot(H_2O)_2]_n$ (**60**)	Hg^{2+}	9.39×10^3	—	112
		$Cr_2O_7^{2-}$	1.16×10^4		
	$[Cd(L_4)(TPOM)_{0.75}]\cdot xG$ (**61**)	Cu^{2+}	1.78×10^4	—	
		$Cr_2O_7^{2-}$	1.34×10^4		
7	$[Zn_8(ad)_4(BPDC)_6O.2Me_2NH_2]\cdot G@DAAC$ (**62**)	CN^-	—	1.93×10^{-8}	113
8	$[Zn(\mu_2\text{-}1Had)(\mu_2\text{-}SO_4)]_n$ (**13**)	Hg^{2+}	7.7×10^3	7.00×10^{-8}	76
9	$\{[Zn(2,5\text{-}tdc)(3\text{-}abit)]\cdot H_2O\}_n$ (**63**)	CrO_4^{2-}	5.43×10^3	—	114
		$Cr_2O_7^{2-}$	5.08×10^3		
10	$\{[Cd(L_{14})(BPDC)]\cdot 2H_2O\}_n$ (**64**)	Fe^{3+}	3.63×10^4	2.21×10^{-6}	115
		CrO_4^{2-}	—	—	
		$Cr_2O_7^{2-}$	6.40×10^3	3.76×10^{-5}	
	$\{[Cd(L_{14})(SDBA)(H_2O)]\cdot 0.5H_2O\}_n$ (**65**)	Fe^{3+}	3.59×10^4	7.14×10^{-6}	
		CrO_4^{2-}	—	—	
		$Cr_2O_7^{2-}$	4.97×10^3	4.86×10^{-5}	
11	$[Cd(4\text{-}tkpvb)(5\text{-}tert\text{-}BIPA)]_n$ (**66**)	Hg^{2+}	1.94×10^4	1.50×10^{-7}	116
		CrO_4^{2-}	4.68×10^4	8.00×10^{-8}	
		$Cr_2O_7^{2-}$	2.50×10^4	1.20×10^{-7}	
12	$\{[Zn(IPA)(L_7)]\}_n$ (**17**)	CrO_4^{2-}	1.00×10^3	1.83×10^{-5}	77
		$Cr_2O_7^{2-}$	1.37×10^3	1.20×10^{-5}	
	$\{[Cd(IPA)(L_7)]\}_n$ (**18**)	CrO_4^{2-}	1.30×10^3	2.52×10^{-6}	
		$Cr_2O_7^{2-}$	2.91×10^3	2.26×10^{-6}	
13	$[Me_2NH_2]_4[Zn_6(qptc)_3(trz)_4]\cdot 6H_2O$ (**67**)	Cr^{3+}	4.39×10^4	1.00×10^{-6}	117
14	$\{[Zn_2(tpeb)_2(2,3\text{-}ndc)_2]\cdot H_2O\}_n$ (**68**)	Cr^{3+}	—	2.19×10^{-9}	118
		CrO_4^{2-}	—	7.23×10^{-9}	
		$Cr_2O_7^{2-}$	—	8.58×10^{-9}	
15	$[Zn(OBA)(DPT)_{0.5}]\cdot DMF$ (**69**)	Hg^{2+}	3.73×10^3	1.80×10^{-6}	119
16	$\{[Zn(ATA)(L_2)]\cdot H_2O\}_n$ (**70**)	CrO_4^{2-}	1.48×10^3	2.50×10^{-7}	120
		$Cr_2O_7^{2-}$	2.62×10^3	4.30×10^{-7}	
		Fe^{3+}	0.55×10^3	3.76×10^{-6}	
		Pd^{2+}	4.18×10^4	2.00×10^{-7}	
	$\{[Cd(ATA)(L_2)]\cdot 2H_2O\}_n$ (**71**)	CrO_4^{2-}	0.97×10^3	1.80×10^{-7}	
		$Cr_2O_7^{2-}$	3.11×10^3	1.90×10^{-7}	
		Fe^{3+}	3.83×10^3	1.77×10^{-6}	
		Pd^{2+}	7.87×10^4	1.00×10^{-7}	
17	$\{[Cd_2(bptc)(2,2'\text{-}bipy)_2(H_2O)_2]\}_n$ (**72**)	Fe^{3+}	8.61×10^3	1.02×10^{-5}	121
		CrO_4^{2-}	7.95×10^3	7.79×10^{-6}	
		$Cr_2O_7^{2-}$	1.17×10^4	7.38×10^{-6}	
	$\{[Cd_2(bptc)(phen)_2]\cdot 4H_2O\}_n$ (**73**)	Fe^{3+}	3.07×10^3	2.17×10^{-5}	
		CrO_4^{2-}	1.09×10^3	1.06×10^{-4}	
		$Cr_2O_7^{2-}$	2.09×10^3	5.89×10^{-5}	
	$\{[Cd_2(bptc)(4,4'\text{-}bipy)(H_2O)_2]\cdot 4H_2O\}_n$ (**74**)	Fe^{3+}	6.21×10^3	2.03×10^{-5}	
		CrO_4^{2-}	5.38×10^3	1.60×10^{-5}	
		$Cr_2O_7^{2-}$	9.34×10^3	1.36×10^{-5}	
18	$\{[Zn_2(1,4\text{-}ndc)_2(3\text{-}abpt)]\cdot 2DMF\}_n$ (**75**)	Fe^{3+}	2.38×10^4	—	122
		Al^{3+}	6.98×10^4	—	
	$\{[Cd(1,4\text{-}ndc)(3\text{-}abit)]\cdot H_2O\}_n$ (**76**)	Fe^{3+}	9.54×10^3	—	
		Al^{3+}	3.84×10^4	—	
19	$\{[Cd(dpb)_2(bimb)_2]\cdot 0.5H_2O\}_n$ (**77**)	$Cr_2O_7^{2-}$	6.25×10^3	—	123
	$[Cd(dpb)(tib)]_n$ (**78**)	Fe^{3+}	1.21×10^4	—	123
		$Cr_2O_7^{2-}$	4.89×10^4	—	
	$[Zn(Hdpb)_2(4,4'\text{-}bibp)]_n$ (**79**)	Fe^{3+}	9.38×10^3	—	
		$Cr_2O_7^{2-}$	4.35×10^4	—	
	$[Cd(dpb)(1,3\text{-}bitl)]_n$ (**80**)	Cu^{2+}	4.89×10^4	—	
		$Cr_2O_7^{2-}$	1.04×10^4	—	

Table 2 *(Contd.)*

Sr no.	LMOFs/LCPs[a]	Inorganic analyte	K_{sv} (M^{-1})	LOD (M)	Ref.
20	$\{[Zn_2(L_8)(L_3)_2]\cdot 3H_2O\}_n$ (**21**)	Fe^{3+}	4.47×10^3	1.29×10^{-6}	79
21	$[Zn_3(L_{10})_2(dpp)_2]_n$ (**30**)	Cu^{2+}	9.70×10^3	1.05×10^{-6}	83
22	Zn(HTABDC)(bpy)·DMF (**81**)	Al^{3+}	—	—	124
23	$\{[Cd_2(HDDB)(bib)_{1.5}(H_2O)]\cdot 2.5H_2O\}_n$ (**82**)	CrO_4^{2-}	4.70×10^3	—	125
		$Cr_2O_7^{2-}$	2.70×10^4	—	
	$[Cd_2(HDDB)(m\text{-}bimb)]\cdot H_2O\}_n$ (**83**)	CrO_4^{2-}	2.50×10^3	—	
		$Cr_2O_7^{2-}$	1.80×10^4	—	
	$\{[Cd_2(DDB)(p\text{-}bimb)]\cdot 2.5H_2O\cdot 0.5(p\text{-}H_2bimb)\}_n$ (**84**)	CrO_4^{2-}	6.00×10^3	—	
		$Cr_2O_7^{2-}$	2.80×10^4	—	
24	$\{[Cd(BIPA)(IPA)]\cdot DMF\}_n$ (**85**)	Hg^{2+}	9.21×10^3	5.0×10^{-7}	126
		Pb^{2+}	—	7.5×10^{-7}	
	$\{[Cd(BIPA)(HIPA)]\cdot DMF\}_n$ (**86**)	Hg^{2+}	1.28×10^4	2.50×10^{-7}	
		Pb^{2+}	—	5.00×10^{-7}	
	$\{[Cd(BIPA)(NIPA)]\cdot 2H_2O\}_n$ (**87**)	Cu^{2+}	—	—	
		Fe^{3+}	—	—	
25	$[Cd_{2.5}(PDA)(trz)_3]_n$ (**88**)	I^-	1.80×10^4	6.30×10^{-7}	127
26	$[Zn(dpdc)(btb)_{0.5}]_n$ (**89**)	Fe^{3+}	—	—	128
		Al^{3+}	—	—	
	$[Cd(dpdc)(btb)_{0.5}]_n$ (**90**)	Fe^{3+}	—	—	
27	$\{[Zn_2(\mu_3\text{-}OH)(cpta)(4,4'\text{-}bipy)]\cdot H_2O\}_n$ (**31**)	Cr^{3+}	9.47×10^3	5.55×10^{-6}	84
		$Cr_2O_7^{2-}$	5.45×10^3	6.91×10^{-6}	
28	$[Cd(TPA)(BIB)]_n$ (**32**)	Hg^{2+}	5.70×10^4	2.10×10^{-7}	85
		$Cr_2O_7^{2-}$	3.60×10^4	1.10×10^{-6}	
	$[Cd(TPA)(BIYB)]_n$ (**33**)	Hg^{2+}	4.60×10^4	1.90×10^{-7}	
		$Cr_2O_7^{2-}$	1.40×10^7	2.40×10^{-7}	
29	$[Cd_2(L_{15})_2(hfpd)]_n$ (**91**)	Fe^{3+}	7.90×10^4	3.10×10^{-7}	129
	$[Zn(L_{15})(tbta)]_n$ (**92**)	Fe^{3+}	8.60×10^4	8.50×10^{-7}	
30	$[Zn_2(mtrb)_2(btec)]\cdot H_2O\}_n$ (**93**)	Fe^{3+}	1.92×10^3	6.28×10^{-7}	130
		CrO_4^{2-}	1.62×10^3	5.72×10^{-7}	
		$Cr_2O_7^{2-}$	4.40×10^3	3.05×10^{-7}	
31	$[Zn_3(bpydb)_2(atz)_2(DMF)](DMF)_6\}_n$ (**94**)	Fe^{3+}	1.15×10^4	—	131
32	$[Cd_3(cpota)_2(phen)_3]_n\cdot 5H_2O$ (**95**)	CrO_4^{2-}	6.90×10^3	3.70×10^{-7}	132
		$Cr_2O_7^{2-}$	1.21×10^4	4.18×10^{-7}	
33	$[Zn_2(BDC)_{1.5}(L_{16})(DMF)]\cdot 1.5DMF$ (**96**)	MnO_4^-	3.20×10^5	3.00×10^{-8}	133
		CrO_4^{2-}	6.10×10^5	3.00×10^{-8}	
		$Cr_2O_7^{2-}$	1.00×10^6	2.00×10^{-8}	
34	$[Cd(2\text{-}bpeb)_{0.5}(CNA)(H_2O)]_n$ (**97**)	MnO_4^-	3.55×10^4	7.79×10^{-5}	134
		$Cr_2O_7^{2-}$	7.61×10^3	3.67×10^{-4}	
	$[Cd(2\text{-}bpeb)_{0.5}(NDC)]_n$ (**98**)	MnO_4^-	2.16×10^4	1.31×10^{-4}	
		$Cr_2O_7^{2-}$	3.10×10^3	9.20×10^{-4}	
	$[Zn(2\text{-}bpeb)(BDC)]_n$ (**99**)	MnO_4^-	1.04×10^4	2.70×10^{-4}	
		$Cr_2O_7^{2-}$	1.88×10^3	1.44×10^{-3}	
35	$[Zn_2(cptpy)(btc)(H_2O)]_n$ (**41**)	Fe^{3+}	3.08×10^3	4.33×10^{-6}	91
36	$[Zn_2(H_2BCA)_2(o\text{-}bimb)_2(H_2O)_2]_n$ (**42**)	CrO_4^{2-}	—	1.30×10^{-7}	92
		$Cr_2O_7^{2-}$	6.6×10^4	7.00×10^{-8}	
	$\{[Zn(H_2BCA)(m\text{-}bib)]\cdot H_2O\}_n$ (**43**)	CrO_4^{2-}	—	1.40×10^{-7}	
		$Cr_2O_7^{2-}$	5.3×10^4	7.00×10^{-8}	
37	$\{[Zn(L_{11})_{0.5}(bimbu)]\cdot 2H_2O\cdot 0.5(CH_3)_2NH\}_n$ (**44**)	Fe^{3+}	6.28×10^4	4.80×10^{-7}	93
		CrO_4^{2-}	5.04×10^4	6.00×10^{-7}	
		$Cr_2O_7^{2-}$	5.68×10^4	5.30×10^{-7}	
37	$\{[Zn(L_{11})_{0.5}(bimb)]\cdot 4H_2O\}_n$ (**45**)	Fe^{3+}	4.07×10^4	7.40×10^{-7}	93
		CrO_4^{2-}	6.76×10^4	4.40×10^{-7}	
		$Cr_2O_7^{2-}$	7.35×10^4	4.10×10^{-7}	
	$\{[Zn(L_{11})_{0.5}(btdpe)]\cdot H_2O\}_n$ (**46**)	Fe^{3+}	5.10×10^4	5.90×10^{-7}	
		CrO_4^{2-}	6.47×10^4	5.40×10^{-7}	
		$Cr_2O_7^{2-}$	5.55×10^4	4.80×10^{-7}	
	$[Zn(L_{11})_{0.5}(bidpe)]_n$ (**47**)	Fe^{3+}	4.67×10^4	6.40×10^{-7}	
		CrO_4^{2-}	5.54×10^4	5.40×10^{-7}	
		$Cr_2O_7^{2-}$	6.20×10^4	4.80×10^{-7}	
38	$\{[Zn(L_{17})(bpeb)]\cdot(DMA)_{2.5}\}_n$ (**100**)	CrO_4^{2-}	0.82×10^4	4.40×10^{-5}	135
		$Cr_2O_7^{2-}$	2.27×10^4	1.60×10^{-5}	
39	$\{[Cd_{1.5}(DBPT)(DiPyDz)(H_2O)]\cdot 3.5H_2O\}_n$ (**101**)	Fe^{3+}	4.78×10^5	1.94×10^{-5}	136

Table 2 *(Contd.)*

Sr no.	LMOFs/LCPs[a]	Inorganic analyte	K_{sv} (M^{-1})	LOD (M)	Ref.
40	$[Zn(afsba)(bbtz)_{1.5}(H_2O)_2]\cdot 2H_2O\}_n$ (**102**)	Fe^{3+}	4.25×10^4	1.29×10^{-6}	137
		CrO_4^{2-}	2.06×10^4	1.90×10^{-6}	
		$Cr_2O_7^{2-}$	4.42×10^4	1.18×10^{-6}	
41	$[Zn(oba)_2(bipy)_2]_n$ (**103**)	Fe^{3+}	2.98×10^4	—	138
		CrO_4^{2-}	—	—	
		$Cr_2O_7^{2-}$	9.26×10^3	—	
42	$\{[Zn_2(L_{18})_2(BDC)]\cdot 2H_2O\}_n$ (**104**)	Fe^{3+}	6.40×10^3	3.84×10^{-6}	139
		CrO_4^{2-}	1.30×10^4	2.10×10^{-6}	
		$Cr_2O_7^{2-}$	6.05×10^3	3.80×10^{-6}	
43	$[Zn_2(oba)_2(bpta)]\cdot(DMF)_3\}_n$ (**105**)	Fe^{3+}	6.50×10^4	3.00×10^{-6}	140
		Al^{3+}	1.40×10^3	1.20×10^{-6}	
44	$[Zn(opda)(bib)]_n$ (**48**)	$Cr_2O_7^{2-}$	1.54×10^7	2.99×10^{-7}	94
	$[Zn(ppda)(bib)(H_2O)]_n$ (**49**)	$Cr_2O_7^{2-}$	9.77×10^8	4.37×10^{-7}	
45	$[Zn(NH_2\text{-}bdc)(4,4'\text{-}bipy)]_n$ (**50**)	CrO_4^{2-}	4.56×10^3	2.21×10^{-6}	95
		$Cr_2O_7^{2-}$	7.62×10^3	1.30×10^{-6}	
46	$\{Zn_2(tpt)_2(tdc)_2\cdot H_2O\}_n$ (**51**)	Fe^{3+}	4.60×10^4	4.72×10^{-6}	96
47	$[Cd_2(2\text{-}abpt)(Hbtca)(H_2btca)_{0.5}(H_2O)]_n$ (**52**)	Cu^{2+}	3.83×10^4	1.39×10^{-6}	97
48	$\{[Zn(L_{19})(bimb)]\cdot 2H_2O\}_n$ (**106**)	Fe^{3+}	1.66×10^5	1.80×10^{-7}	141
		CrO_4^{2-}	4.94×10^4	6.10×10^{-7}	
		$Cr_2O_7^{2-}$	—	—	

[a] L_{12} = hexa[4-(carboxyphenyl)oxamethyl]-3-oxapentane acid; bipy = 2,2′-bipyridine or 4,4′-bipyridine; bibp = 4,4′-di(1*H*-imidazol-1-yl)-1,1′-biphenyl; tib = 1,3,5-tri(1*H*-imidazol-1-yl)benzene; L_{13} = 4,4′-((1,2-phenylenebis(methylene))bis(oxy))dibenzoic acid; bpe = (*E*)-1,2-di(pyridin-4-yl)ethene; 2-NH_2bdc or ATA = 2-amino-1,4-benzenedicarboxylic acid; hfipbb = 4,4-(hexafluoroisopropylidene)bis(benzoic acid); trz = triazole; 5-asba = 2-amino-5-sulfobenzoic acid; bimbu = 1,4-bis(1*H*-imidazol-1-yl)butane; L_4 = benzo-(1,2;4,5)-bis(thiophene-2′-carboxylic acid; BBI = 1,1′-(1,4-butanediyl)bis(imidazole); TPOM = tetrakis(4-pyridyloxy-methylene) methane; BPDC = biphenyl dicarboxylic acid; ad = adenine; DAAC = 3,6-diaminoacridinium cation; 2,5-tdc = 2,5-thiophenedicarboxylic acid; 3-abit = 4-amino-3,5-bis(imidazol-1-ylmethyl)-1,2,4-triazole; L_{14} = 4,4′-(2,5-bis-(methylthio)-1,4-phenylene)dipyridine; SDBA = 4,4′-sulfonyldibenzoic acid; 4-tkpvb = 1,2,4,5-tetrakis(4-pyridylvinyl)benzene; 5-*tert*-BIPA = 5-*tert*-butylisophthalic acid; IPA = isophthalic acid; L_7 = 3-pyridylcarboxaldehyde nicotinoylhydrazone; qptc = terphenyl-2,5,2′5′-tetracarboxylic acid; tpeb = 1,3,5-tri-4-pyridyl-1,2-ethenylbenzene; ndc = naphthalenedicarboxylic acid; OBA = 4,4′-oxybis(benzoic acid); DPT = 3,6-di(pyridin-4-yl)-1,2,4,5-tetrazine; L_2 = 4-pyridyl carboxaldehyde isonicotinoylhydrazone; bptc = 3,3′,5,5′-biphenyltetracarboxylic acid; phen = 1,10-phenanthroline; abpt = 4-amino-3,5-bis(3-pyridyl)-1,2,4-triazole or 3,5-di(2 -pyridyl)-4-amino-1,2,4-triazole; bimb = 1,4-bis(imidazol-1-ylmethyl)benzene; 1,3-bitl = 1,3-bis(1-imidazoly)toluene; dpb = 3,5-di(4′-carboxyl-phenyl)benzene acid; L_3 = 5-aminoisophthalic acid; L_8 = 3-pyridin-3-yl-*N*-[5-(3-pyridin-3-yl-acryloylamino)-naphthalen-1-yl]-acrylamide; L_{10} = 3,5-dibromosalicylaldehyde salicylhydrazone; dpp = 1,3-di(4-pyridyl)propane; HTABDC = 4,4′-((*Z*,*Z*)-1,4-diphenylbuta-1,3-diene-1,4-diyl)bis(2-hydroxybenzoic acid); DDB = 3,5-di(2′,4′-dicarboxylphenyl)benozoic acid; bib = 1,4-bis(imidazol-1-yl)benzene; BIPA = bis(4-(1*H*-imidazol-1-yl)phenyl)amine; HIPA = 5-hydroxyisophthalic acid; NIPA = 5-nitroisophthalic acid; PDA = 1,4-phenylenediacetate; dpdc = 3,3′-diphenyldicarboxylate; btb = 1,4-bis(1,2,4-triazol-1-yl)butane; cpta = 2-4(-carboxyphenoxy)terephthalic acid; TPA = 3,3′-thiodipropionic acid; BIYB = 4,4-bis(imidazol-1-ylmethyl)biphenyl; L_{15} = 1,5-bis(2-methylbenzimidazol-1-yl)pentane; hfpd = 4,4′-(hexafluoroisopropylidene)diphthalic acid; tbta = tetrabromoterephthalic acid; bpydb = 4,4′-(4,4′-bipyridine-2,6-diyl)dibenzoic acid; atz = 3-amino-1,2,4-triazole; cpota = 2-(4-carboxyphenoxy)terephthalic acid; L_{16} = pyridine 4-carboxylic acid; BDC = benzene-1,4-dicarboxylate; CNA = 4-carboxycinnamic acid; bpeb = 2-(4-((*E*)-2-(pyridine-2-yl)vinyl)styryl)-pyridine or 1,4-bis[2-(4-pyridyl)ethenyl]benzene; cptpy = 4-(4-carboxyphenyl)-2,2′:4′,4″-terpyridine; btc = 1,3,5-benzenetricarboxylic acid; BCA = bis(4-carboxybenzyl)amine; L_{11} = 5,5′-(1,4-xylylenediamino)diisophthalic acid; btdpe = 4,4′-bis(4*H*-1,2,4-triazol-4-yl)diphenyl ether; bidpe = 4,4′-bis(imidazolyl)diphenyl ether; L_{17} = 4,4′-((1,3-phenylenebis(methylene))bis(oxy))dibenzoic acid; DBPT = 3-(3,5-dicarboxylphenyl)-5-(4-carboxylphenyl)-1*H*-1,2,4-triazole; DiPyDz = 1,2-di(pyridin-4-yl)diazene; afsba = 2-amino-5-sulfobenzoic acid; bbtz = 1,4-bis(triazol-1-ylmethyl)benzene; L_{18} = 4-(tetrazol-5-yl)phenyl-4,2′:6′,4″-terpyridine; bpta = N^1,N^4-di(pyridin-4-yl)terephthalamide; opda = 1,2-phenylenediacetic acid; ppda = 1,4-phenylene-diacetic acid; tpt = 2,4,6-tri(pyridin-4-yl)-1,3,5-triazine; btca = 1,2,4,5-Benzenetetracarboxylic.

stants 6.40×10^3 M^{-1} (**64**), 4.97×10^3 M^{-1} (**65**) and LOD values 3.76×10^{-5} M (**64**), 4.86×10^{-5} M (**65**) respectively. Similarly, both LMOFs detect Fe^{3+} with K_{sv} 3.59×10^4 M^{-1} (**64**), 3.63×10^4 M^{-1} (**65**) and LOD values 2.21×10^{-6} M (**64**), 7.14×10^{-6} M (**65**) respectively. The quenching mechanism is proposed based on competition between analytes and LMOFs for absorption energy due to a similar absorbance region.[115] Lang and coworkers constructed a dual ligand luminescent coordination polymer $[Cd(4\text{-tkpvb})(5\text{-}tert\text{-BIPA})]_n$ (**66**) from N-donor 4-tkpvb (1,2,4,5-tetrakis(4-pyridylvinyl)benzene) and dicarboxylate 5-*tert*-BIPA (5-*tert*-butylisophthalic acid). LCP (**66**) acts as an aqueous phase multi-responsive fluorosensor for chromate anions and mercury cations. Excellent quenching constants 1.94×10^4 M^{-1} (Hg^{2+}), 4.68×10^4 M^{-1} (CrO_4^{2-}), 2.50×10^4 M^{-1} ($Cr_2O_7^{2-}$) and detection limit values 1.50×10^{-7} M (Hg^{2+}), 8.00×10^{-8} M (CrO_4^{2-}), 1.20×10^{-7} M ($Cr_2O_7^{2-}$) for LCP (**66**) demonstrated the selective and sensitive detection of these analytes. The sensing mechanism was explicated by the interaction of analytes with a free pyridyl moiety and energy transfer between analyte/LCP.[116] Formerly mentioned multi-responsive LCPs (**17**) and (**18**) also displayed selectivity towards chromate/dichromate anions with quenching constants 1.00×10^3/1.37×10^3 M^{-1} (**17**) and 1.30×10^3/2.91×10^3 M^{-1} among other inorganic anions (Fig. 10). Detection limits for chromate/dichromate anions were 1.83×10^{-5}/1.20×10^{-5} M (**17**) and 2.52×10^{-6}/2.26×10^{-6} M (**18**) suggesting good sensitivity

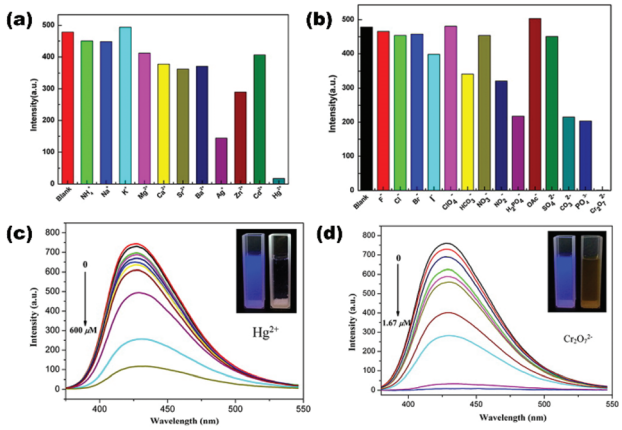

Fig. 8 (a and b) Quenching effect on the fluorescence intensity of (**57**) by various cations/anions in the aqueous phase; (c and d) fluorescence spectra of (**57**) in the presence of increasing concentration of Hg^{2+} and $Cr_2O_7^{2-}$. Inset: Visual changes of quenching effect under UV light (365 nm). Reproduced with permission from ref. 110. Copyright 2015 American Chemical Society.

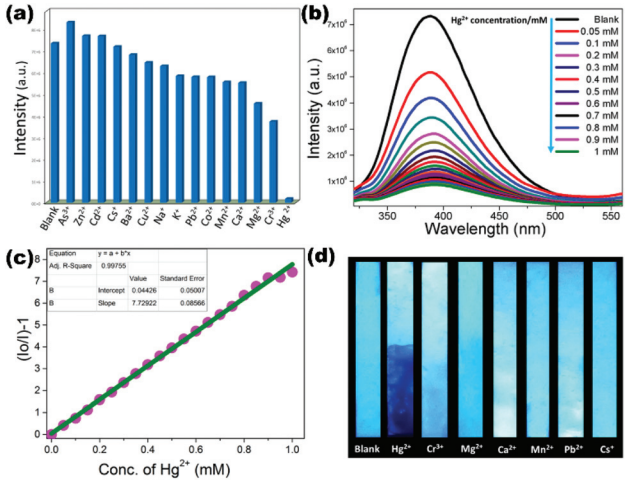

Fig. 9 (a) Emission quenching (%) of (**13**) upon addition of different cations; (b) emission behavior of (**13**) dispersed in water toward different concentrations of Hg^{2+}; (c) Stern–Volmer plots for (**13**) upon gradual addition of Hg^{2+} solution; (d) digital images of (**13**)-coated test strips after they were dipped in aqueous solutions of cations. Reproduced with permission from ref. 74. Copyright 2017 American Chemical Society.

towards these analytes. Competition for excitation energy between analytes/LCPs and energy transfer supported by spectral overlap between analytes/LCPs are the main justification for the sensing mechanism.[77]

Mixed linker 3D luminescent MOF $[Me_2NH_2]_4[Zn_6(qptc)_3(trz)_4]\cdot 6H_2O$ (**67**) constructed using π-conjugated dicarboxylate qptc (terphenyl-2,5,2′5′-tetracarboxylic acid) and N-heterocycle triazole exhibits high fluorescence properties towards sensing of the chromium cation (Cr^{3+}) in water with K_{sv} 4.39 × 10^4 M^{-1} and LOD value 1.00 × 10^{-6} M. Supramolecular interaction of the analyte with uncoordinated carboxylate oxygen on LMOF (**67**) is responsible for the fluorescence quenching mechanism.[117] Fluorescence sensing for chromate anions as well as chromium cations in the aqueous phase by Zn(II) based luminescent coordination polymer $\{[Zn_2(tpeb)_2(2,3\text{-ndc})_2]\cdot H_2O\}_n$ (**68**) engaging N-donor tpeb (1,3,5-tri-4-pyridyl-1,2-ethenylbenzene) and naphthalene dicarboxylate (2,3-ndc) is reported by Lang *et al.* Excellent sensitivity supported by a higher limit of detection values 2.19 × 10^{-9} M (Cr^{3+}), 7.23 × 10^{-9} M (CrO_4^{2-}), 8.58 × 10^{-9} M ($Cr_2O_7^{2-}$) and quenching is inferred by an energy transfer phenomenon *via* a spectral overlap of analyte/LCP.[118] Mixed linker fluorescent MOF $[Zn(OBA)(DPT)_{0.5}]\cdot DMF$ (**69**) synthesized by Morsali and co-workers from flexible dicarboxylate OBA (4,4′-oxybis(benzoic acid)) and tetrazine functionalized N-donor DPT (3,6-di(pyridin-4-yl)-1,2,4,5-tetrazine) showed excellent turn on fluorescence sensing properties for Hg^{2+} in water with enhancement constant 3.73 × 10^3 M^{-1} and lower detection value 1.80 × 10^{-6} M.[119] Two 3D dual ligand LMOFs $\{[Zn(ATA)(L_2)]\cdot H_2O\}_n$ (**70**) and $\{[Cd(ATA)(L_2)]\cdot 2H_2O\}_n$ (**71**) constructed using amino functionalized dicarboxylate ATA (2-amino-1,4-benzenedicarboxylic acid) and Schiff base N-donor pillar L_2 (4-pyridyl carboxaldehyde isonicotinoylhydrazone) by us possess excellent photoluminescence in the solid-state as well as in water revealing a selective multisensory material towards inorganic pollutants (CrO_4^{2-}, $Cr_2O_7^{2-}$, Fe^{3+} and Pd^{2+}). Water stable LMOFs showed high quenching ability for $CrO_4^{2-}/Cr_2O_7^{2-}$ anions with K_{sv} values 1.48 × 10^3/2.62 × 10^3 M^{-1} (**70**), 0.97 × 10^3/3.11 × 10^3 M^{-1} (**71**) and detection limit values 2.50 × 10^{-7}/4.30 × 10^{-7} M, 1.80 × 10^{-7}/1.90 × 10^{-7} M (**71**) respectively (Fig. 11). Similarly, both LMOFs also demonstrated sensing ability for Fe^{3+}/Pd^{2+} cations with K_{sv} values 0.55 × 10^3/4.18 × 10^4 M (**70**), 3.83 × 10^3/7.87 × 10^4 M^{-1} (**70**), 3.76 × 10^{-6}/2.00 × 10^{-7} M^{-1} (**71**) and LOD values 3.76 × 10^{-6}/2.00 × 10^{-7} M (**70**), 1.77 × 10^{-6}/1.00 × 10^{-7} M (**71**) respectively. The sensing mechanism was explained by the interaction of analytes with a free amino group/amide group on linkers and energy transfer *via* spectral overlap between analyte/LMOFs.[120]

Three cadmium based dual linker LCPs $\{[Cd_2(bptc)(2,2'\text{-bipy})_2(H_2O)_2]\}_n$ (**72**), $\{[Cd_2(bptc)(phen)_2]\cdot 4H_2O\}_n$ (**73**) and $\{[Cd_2(bptc)(4,4'\text{-bipy})(H_2O)_2]\cdot 4H_2O\}_n$ (**74**) were synthesized from 3,3′,5,5′-biphenyltetracarboxylate (bptc) in combination with different pyridyl based N-donor spacers. All LCPs selectively detect chromate anions and Fe^{3+} cations in the aqueous phase with quenching constant values nearer to 10^3 M^{-1} and LOD values nearer to 10^{-5} M (Table 2, entry 17).[121] Zhang *et al.* synthesized two LMOFs $\{[Zn_2(1,4\text{-ndc})_2(3\text{-abpt})]\cdot 2DMF\}_n$ (**75**) and $\{[Cd(1,4\text{-ndc})(3\text{-abit})]\cdot H_2O\}_n$ (**76**) and successfully utilized as multi-responsive fluorosensors for Fe^{3+}/Al^{3+} in the aqueous phase with excellent quenching constant values (Table 2, entry 18).[122] Similarly, Fan and co-workers reported a series of LCPs $\{[Cd(dpb)_2(bimb)_2]\cdot 0.5H_2O\}_n$ (**77**), $[Cd(dpb)(tib)]_n$ (**78**), $[Zn(Hdpb)_2(4,4'\text{-bibp})]_n$ (**79**) and $[Cd(dpb)(1,3\text{-bitl})]_n$ (**80**) constructed from V-shaped 3,5-di(4′-carboxyl-phenyl)benzene acid (dpb) in combination with various imidazole based N-donor linkers. All LCPs exhibit fluorescence properties in water and developed as multisensory materials towards various inorganic pollutants (Table 2, entry 19).[123]

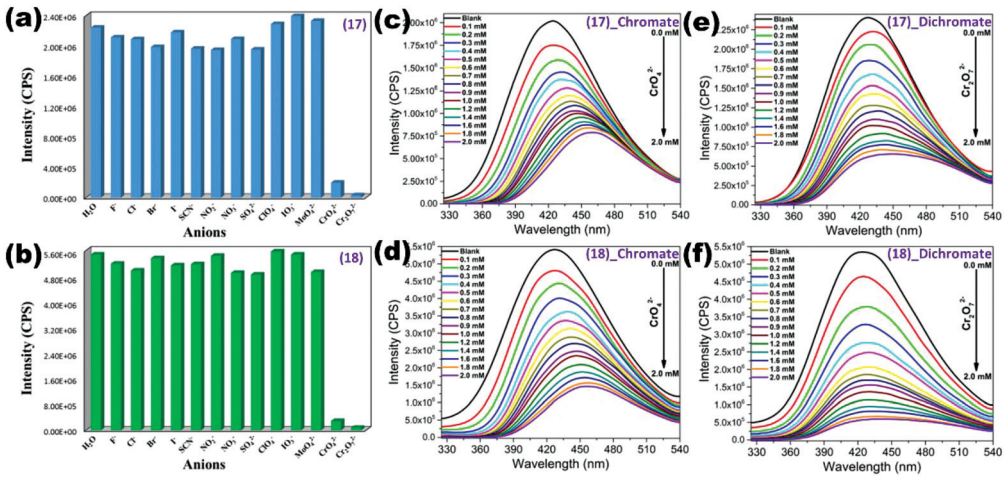

Fig. 10 (a and b) Quenching efficiency of (**17**) and (**18**) for different anions; (c, d, e and f) Fluorescence titration of (**17**) and (**18**) (dispersed in water) for different concentrations of chromate anions. Reproduced with permission from ref. 77. Copyright 2017 American Chemical Society.

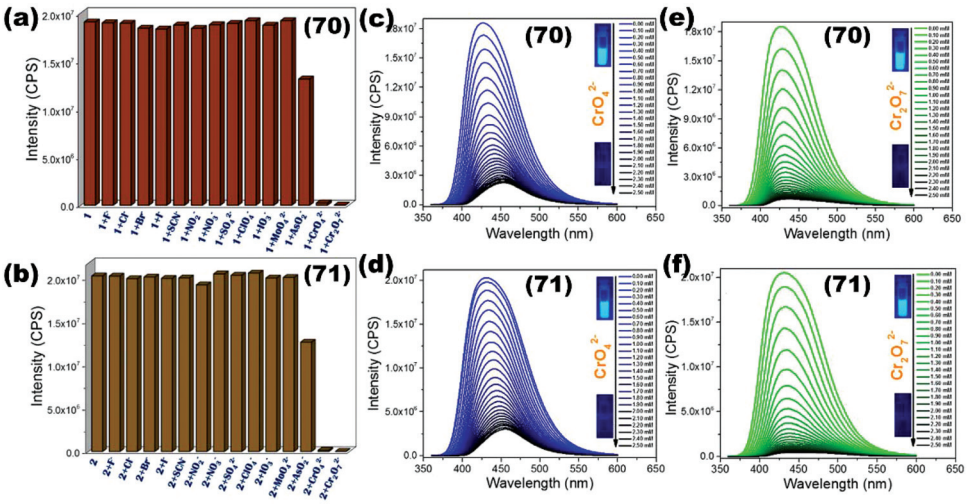

Fig. 11 (a and b) Fluorescence quenching effect of different aqueous anion solutions on LMOFs (**70**) and (**71**); (c–f) luminescence titration of (**70**) and (**71**) by increasing concentration of CrO_4^{2-}/$Cr_2O_7^{2-}$ solutions in water. Reproduced with permission from ref. 120. Copyright 2017 American Chemical Society.

LCP (**21**) formerly discussed as a fluorosensor for organic pollutants is also exploited as a luminescent sensory material towards the Fe^{3+} cation with K_{sv} value 4.47×10^3 M^{-1} and LOD value 1.29×10^{-6} M in water.[79] Similarly, LCP (**30**) demonstrated excellent aqueous phase sensing behaviour for Cu^{2+} with quenching constant 9.70×10^3 M^{-1} and a detection limit of 1.05×10^{-6} M.[83] Aggregation-induced emission (AIE) active MOF Zn(HTABDC)(bpy)·DMF (**81**) containing 4,4′-((*Z*,*Z*)-1,4-diphenylbuta-1,3-diene-1,4-diyl)bis(2-hydroxybenzoic acid) (HTABDC) and bipyridyl linker demonstrated fluorescence turn on sensing of the Al^{3+} cation in water.[124] Three mixed ligand LMOFs $\{[Cd_2(HDDB)(bib)_{1.5}(H_2O)]\cdot 2.5H_2O\}_n$ (**82**), $[Cd_2(HDDB)(m\text{-}bimb)]\cdot H_2O\}_n$ (**83**) and $\{[Cd_2(DDB)(p\text{-}bimb)]\cdot 2.5H_2O\cdot 0.5(p\text{-}H_2bimb)\}_n$ (**84**) synthesized from 3,5-di(2′,4′-dicarboxylphenyl)benzoic acid (DDB) and imidazole based N-donor spacers have been exploited for the aqueous phase detection of chromate anions. The emission intensity of LMOFs selectively quenches by chromate and dichromate solution with the K_{sv} value in the range 10^3–10^4 M^{-1} (Table 2, entry 23).[125] Zheng *et al.* reported the synthesis and luminescence properties of three dual linker Cd(II) MOFs $\{[Cd(BIPA)(IPA)]\cdot DMF\}_n$ (**85**), $\{[Cd(BIPA)(HIPA)]\cdot DMF\}_n$ (**86**) and $\{[Cd(BIPA)(NIPA)]\cdot 2H_2O\}_n$ (**87**) coined from angular isophthalic acid derivatives and imidazole based N-donor spacer 1,4-bis(imidazol-1-ylmethyl)benzene (bimb). All LMOFs showed different degrees of quenching and enhancement behaviour for different metal ions in the aqueous phase. LMOFs (**85**) and (**86**) remained sensitive for Hg^{2+} *via* a turn off and Pb^{3+} *via* a turn on phenomenon (Fig. 12), whereas LMOF (**87**) showed quenching ability towards Fe^{3+} and Cu^{2+} (Table 2, entry 24).[126]

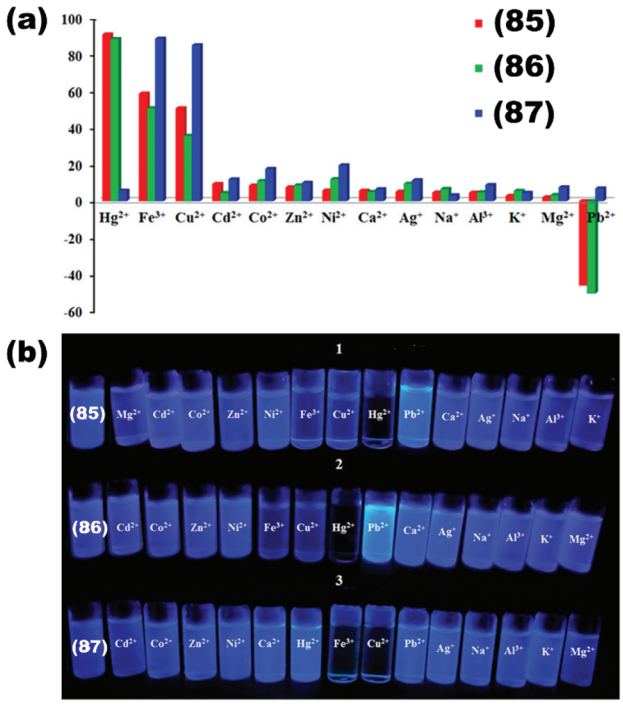

Fig. 12 (a) Quenching percentage of (85–87) in the presence of different metal ion solutions, (b) digital images blank (85–87) and after addition of different metal ion solutions under UV light (310 nm). Reproduced with permission from ref. 126. Copyright 2018 American Chemical Society.

Mahata and co-workers reported iodide (I^-) sensing by mixed ligand LMOF $[Cd_{2.5}(PDA)(trz)_3]_n$ (**88**) containing 1,4-phenylenediacetic acid (PDA) and 1,2,4-triazole in water.

LMOF (**88**) showed excellent quenching ability for iodide with K_{sv} value 1.80×10^4 M^{-1} and lower detection limit 6.30×10^{-7} M among other anions. The sensing mechanism was explained by the molecular interaction of iodide with LMOF and unsaturation present in the penta-coordinated Cd(II) metal centre.[127] Two luminescent MOFs $[Zn(dpdc)(btb)_{0.5}]_n$ (**89**) and $[Cd(dpdc)(btb)_{0.5}]_n$ (**90**) prepared using diphenyldicarboxylate (dpdc) and N-donor spacer 1,4-bis(1,2,4-triazol-1-yl)butane (btb) showed aqueous luminescence sensing behaviour towards Fe^{3+} and Al^{3+} cations *via* interaction with free N-atoms on the framework.[128] LMOF (**31**) also acts as a multi-responsive sensing material for $Cr^{3+}/Cr_2O_7^{2-}$ with Stern–Volmer constant value $9.47 \times 10^3/5.45 \times 10^3$ M^{-1} and LOD value $5.55 \times 10^{-6}/6.91 \times 10^{-6}$ M in water.[84] As mentioned in earlier discussions, LMOFs (**32**) and (**33**) are also exploited for the sensing application of $Hg^{2+}/Cr_2O_7^{2-}$ in aqueous media with K_{sv} value $5.70 \times 10^4/3.60 \times 10^4$ M^{-1} (**32**), $4.60 \times 10^4/1.40 \times 10^7$ M^{-1} (**33**) and detection limit values of $2.10 \times 10^{-7}/1.10 \times 10^{-6}$ M (**32**), $1.9 \times 10^{-7}/2.4 \times 10^{-7}$ M (**33**) respectively. The interaction of a thio group present on LMOFs with Hg^{2+} and energy transfer between the accepter (chromate anion) and donor (LMOFs) are responsible factors for the sensing mechanism.[85] LCPs $[Cd_2(L_{15})_2(hfpd)]_n$ (**91**) and $[Zn(L_{15})(tbta)]_n$ (**92**) reported by Cui *et al.* showed Fe^{3+} sensing behaviour with excellent quenching constant $7.90 \times 10^4/8.60 \times 10^4$ M^{-1} and lower detection value $3.10 \times 10^{-7}/8.50 \times 10^{-7}$ M,[129] whereas LCP $[Zn_2(mtrb)_2(btec)]\cdot H_2O\}_n$ (**93**) was exploited as a multifunctional sensory material towards Fe^{3+} and chromate anions in water (Table 2, entry 30).[130] Similarly, dual ligand LMOF $[Zn_3(bpydb)_2(atz)_2(DMF)](DMF)_6\}_n$ (**94**) showed luminescence sensing of Fe^{3+} in water with quenching constant value 1.15×10^4 M^{-1}.[131] 3D microporous mixed ligand LMOF $[Cd_3(cpota)_2(phen)_3]_n\cdot 5H_2O$ (**95**) synthesized from 2-(4-carboxyphenoxy)terephthalic acid (cpota) and 1,10-phenanthroline showed luminescence behavior in water. LMOF (**95**) is applicable for the sensing of hexavalent chromate anions *via* emission quenching with an energy transfer mechanism (Table 2, entry 32).[132]

Recently, Morsali *et al.* reported a water stable 3D dual ligand LMOF $[Zn_2(BDC)_{1.5}(L_{16})(DMF)]\cdot 1.5DMF$ (**96**) constructed from benzene dicarboxylate (BDC)/pyridine carboxylate (L_{16}) and developed a fluorescent chemo sensor for the selective detection of Cr^{VI} and Mn^{VII} oxoanions in the aqueous phase with good recyclability. The emission intensity of LMOF (**96**) was quenched by $MnO^{4-}/CrO_4^{2-}/Cr_2O_7^{2-}$ with excellent K_{sv} values $3.20 \times 10^5/6.10 \times 10^5/1.00 \times 10^6$ M^{-1} and demonstrated higher LOD values $3.00 \times 10^{-8}/3.00 \times 10^{-8}/2.00 \times 10^{-8}$ M. Absorbance bands of the analytes hugely overlapping with the absorbance/emission band of the LMOF clearly suggest the quenching mechanism based on the energy transfer phenomenon.[133] Similarly, three water stable LCPs $[Cd(2\text{-bpeb})_{0.5}(CNA)(H_2O)]_n$ (**97**), $[Cd(2\text{-bpeb})_{0.5}(NDC)]_n$ (**98**) and $[Zn(2\text{-bpeb})(BDC)]_n$ (**99**) synthesized using N-donor spacer 2-(4-((E)-2-(pyridin-2-yl)vinyl)styryl)-pyridine (2-bpeb) along with different dicarboxylates showed sensing affinity towards $MnO^{4-}/Cr_2O_7^{2-}$ anions in water. All three LCPs possess selectivity for $MnO^{4-}/Cr_2O_7^{2-}$ with quenching constant values $3.55 \times 10^4/7.61 \times 10^3$ M^{-1} (**97**), $2.16 \times 10^4/3.10 \times 10^3$ M^{-1} (**98**), $1.04 \times 10^4/1.88 \times 10^3$ M^{-1} (**99**) and detection limit values of $7.79 \times 10^{-5}/3.67 \times 10^{-4}$ M (**97**), $1.31 \times 10^{-4}/9.20 \times 10^{-4}$ M (**98**), $2.70 \times 10^{-4}/1.44 \times 10^{-3}$ M (**99**) respectively. As discussed earlier, the quenching mechanism is supported by competition for excitation energy and energy transfer between analyte/LCPs.[134] LMOF (**41**) mentioned in our earlier readings also had the ability for selective and sensitive sensing of Fe^{3+} cations in water. The sensing ability of LMOF (**41**) is well supported by an energy transfer phenomenon between the donor and accepter with quenching constant 3.08×10^3 M^{-1} and LOD value 4.33×10^{-6} M.[91] Multi-responsive LCPs (**42**) and (**43**) also demonstrated excellent fluorescence quenching properties towards chromate anions with K_{sv} values 6.6×10^4, 5.3×10^4 M^{-1} and LOD values 7.00×10^{-8}, 7.00×10^{-8} M respectively.[92] Likewise, multifunctional LMOFs (**44–47**) showed aqueous phase sensing for Fe^{3+} and chromate oxyanions with sensible quenching constant and limit of detection values (Table 2, entry 37). Spectral overlap between analyte/LMOFs suggests that the energy transfer mechanism as well as similar absorbance bands also supported competition for excitation energy resulting in a decrease of emission of LMOFs.[93]

Dual linker 3D pillar-layered LCP $\{[Zn(L_{17})(bpeb)]\cdot(DMA)_{2.5}\}_n$ (**100**) constructed from 4,4′-((1,3-phenylenebis

(methylene))bis(oxy))dibenzoic acid (L_{17}) and N-donor pillar bpeb showed excellent luminescence behaviour in aqueous media and successfully applied for sensitive chromate detection among other interfering anions. The quenching ability of LCP (**100**) for $CrO_4^{2-}/Cr_2O_7^{2-}$ was demonstrated by Stern–Volmer constant values $0.82 \times 10^4/2.27 \times 10^4$ M^{-1} and LOD values of $4.40 \times 10^{-5}/1.60 \times 10^{-5}$ M. LCP (**100**) dispersed in water as well as coated on a paper strip showed visible luminescence reduction upon the addition of chromate anion solution under 365 nm UV radiation (Fig. 13). The sensing mechanism involves the energy transfer *via* spectral overlap of a wide absorbance band of the analyte with an excitation/emission band of LCP.[135] Liu and co-workers synthesized LMOF $\{[Cd_{1.5}(DBPT)(DiPyDz)(H_2O)]\cdot 3.5H_2O\}_n$ (**101**) containing triazole based dicarboxylate DBPT (3-(3,5-dicarboxylphenyl)-5-(4-carboxylphenyl)-1*H*-1,2,4-triazole) and N-donor pillar 1,2-di(pyridin-4-yl)diazene (DiPyDz). LMOF (**101**) possesses luminescence sensing ability for Fe^{3+} cations in water with a quenching constant of 4.78×10^5 M^{-1} and an LOD value of 1.94×10^{-5} M.[136] A series of mixed ligand Zn-based LCPs involving aromatic dicarboxylate and N-donor ligands such as $[Zn(afsba)(bbtz)_{1.5}(H_2O)_2]\cdot 2H_2O\}_n$ (**102**), $[Zn(oba)_2(bipy)_2]_n$ (**103**) and $\{[Zn_2(L_{18})_2(BDC)]\cdot 2H_2O\}_n$ (**104**) with hydrolytic stability have been reported. All three LCPs (**102–104**) showed excellent luminescence properties in water and were successfully utilized as selective sensory materials for the detection of Fe^{3+} cations/chromate oxyanions (Table 2, entries 40–42). The sensing mechanism for all three complexes involves the energy transfer phenomenon between the accepter analyte and donor frameworks.[137–139] Mixed linker Zn(II) MOF $[Zn_2(oba)_2(bpta)]\cdot(DMF)_3\}_n$ (**105**) containing flexible dicarboxylate (oba) and amide functionalized N-donor pillar bpta (N^1,N^4-di(pyridin-4-yl)terephthalamide) verified the selective and sensitive fluorescence sensing ability for Fe^{3+} (turn off) and Al^{3+} (turn on) cations in aqueous media (Table 2, entry 43).[140]

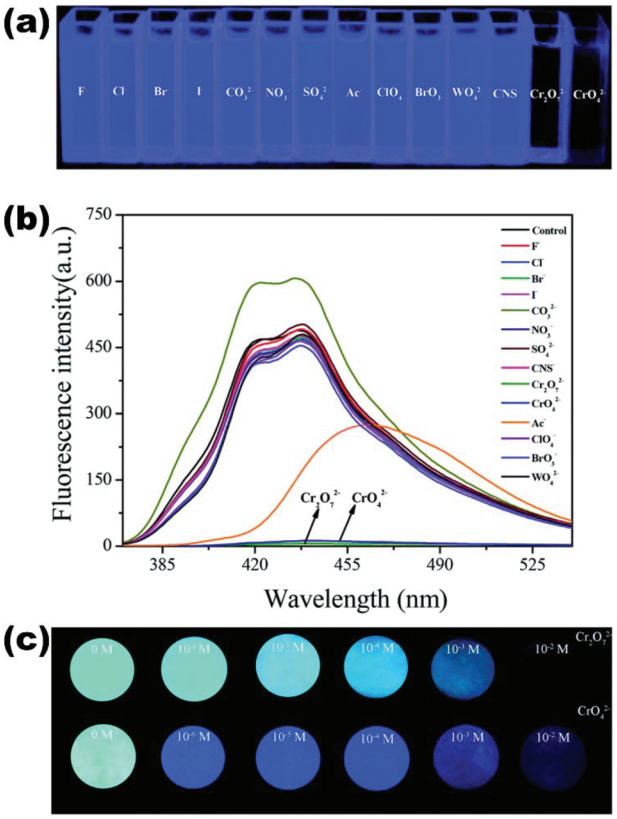

Fig. 13 (a) Digital images of (**100**) in the presence of different anions under a 365 nm UV lamp; (b) fluorescence spectra of (**100**) dispersed in an aqueous solution of different anions; (c) images of (100) coated test paper after immersion in different concentrations of chromate anion solutions under 365 nm UV light. Reproduced with permission from ref. 135. Copyright 2019 Royal Society of Chemistry.

LCPs (**48**) and (**49**) mentioned earlier as sensors of organic pollutants are also applicable as dichromate sensors in water. Fluorescence quenching experiments for both LCPs in the presence of different anions showed the selectivity towards dichromate anions with excellent K_{sv} values 1.54×10^7 M^{-1} (**48**) and 9.77×10^8 M^{-1} (**49**), whereas the sensitivity of LCPs demonstrated lower detection limit values of 2.99×10^{-7} M (**48**), 4.37×10^{-7} M (**49**). The quenching mechanism was supported by the energy transfer process through spectral overlap between the analyte and LCPs.[94] Likewise, amino functionalized dual linker Zn(II) based LMOF (**50**) discussed earlier is also valid as a multi-responsive sensory material towards Cr^{VI} oxyanions in aqueous media. Chromate oxyanions selectively reduced the emission properties of LMOF (**50**) which can also be visible under UV radiation (Fig. 14). Fluorescence titration showed linear behaviour of the Stern–Volmer plot and the respective calculated quenching constant 4.56×10^3 M^{-1} (CrO_4^{2-}) and 7.62×10^3 M^{-1} ($Cr_2O_7^{2-}$) and excellent LOD values of 2.21×10^{-6} M (CrO_4^{2-}) and 1.30×10^{-6} M ($Cr_2O_7^{2-}$) (Fig. 14). The sensing mechanism is clarified by the resonance energy transfer effect and competitive absorption between chromate anions and LMOF (**50**).[95] LMOFs (**51**) and (**52**) also showed the multi sensing properties for Fe^{3+} and Cu^{2+} cations among other interfering cations in water respectively in addition to the sensing of organic pollutants (Table 2, entries 46 and 47).[96,97]

In recent report, Long *et al.* demonstrated the synthesis and sensing properties of a dual ligand luminescent coordination polymer $\{[Zn(L_{19})(bimb)]\cdot 2H_2O\}_n$ (**106**) towards Fe^{3+} cations and chromate anions. The selective detection ability of LCP (**106**) for Fe^{3+}/CrO_4^{2-} is also supported by excellent corresponding quenching constants $1.66 \times 10^5/4.94 \times 10^4$ M^{-1} and LOD values $1.80 \times 10^{-7}/6.10 \times 10^{-7}$ M. Competition for excitation energy between the analyte and LMOF due to a large overlap of absorbance/emission bands is specified to be the probable reason for selective sensing.[141] This section of the review gives a snapshot of various Zn(II)/Cd(II) based mixed ligand fluorosensors which are highly stable in water and showed selective and sensitive detection of various inorganic pollutants in the aqueous phase. The detection of analytes by LMOFs is centred by turn on and turn off fluorescent response and can be accounted for by the interaction of analytes with the fluorophore. The detection of analytes by the LMOF is a

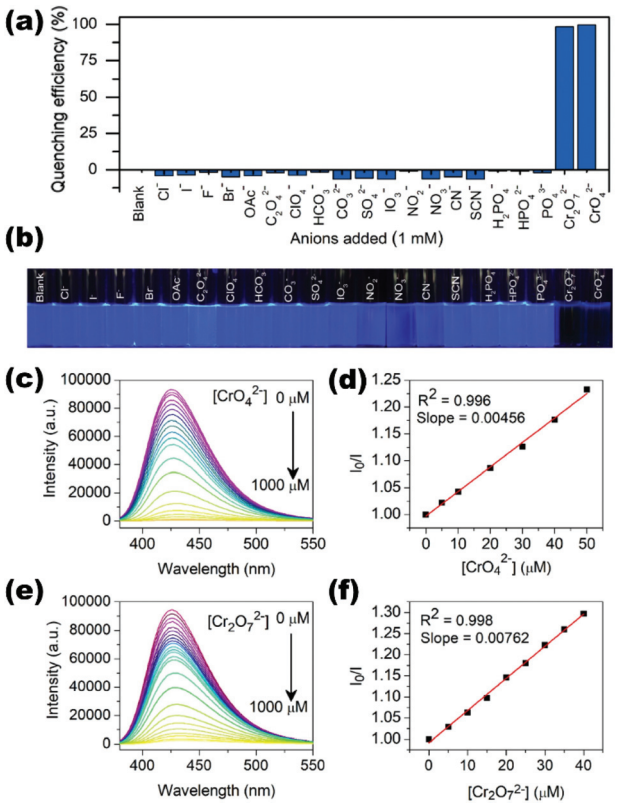

Fig. 14 (a) Quenching percentage of (**50**) dispersed in different anion solutions; (b) digital images of (**50**) dispersed in different anion solutions under UV irradiation; (c and e) fluorescence spectra of (**50**) at different concentrations of chromate anion solutions; (d and f) linear fitting of the Stern–Volmer plot for (**50**) in the presence of chromate anions. Reproduced with permission from ref. 95. Copyright 2019 Elsevier B.V.

well established mechanism based on photoinduced electron transfer (PET), resonance energy transfer (RET) and competition of the excitation energy by the analyte and fluorophore. In most cases of the present investigation, fluorescence quenching is responsible for the detection of both organic and inorganic pollutants and a few and the above-mentioned established mechanisms are responsible for the efficient sensing of diversity of analytes.[18,26] Extensive literature search has been done and most of the results are not only tabulated in the format, we also elaborated the ligands used for the construction of the LCPs, probable sensing mechanism in operation and limit of detection of the pollutants by a variety of LCPs fabricated for fluorescence sensing application.

Conclusions

The past two decades have witnessed rapid development of LMOF/LCP based fluorosensors for numerous chemical species. The studies have shown that the judiciously chosen metal nodes and linkers could not only yield LMOFs/LCPs suitable for chemical sensing but can also impart aquatic and chemical stability to the framework, which paves the way for their in-field applications. Critical evaluation of relevant research testifies that the photoluminescence of MOFs is not only sensitive to the nature of their constituent metal nodes and linkers but also to the structure of the chemical entities in their surroundings by virtue of delicate host–guest interactions. This fact has been exploited by researchers to develop fluorosensors suitable for sensitive detection of noxious organic and inorganic pollutants species present in polluted water. In this review we have provided an up-to-date account of Zn(II)/Cd(II) and mixed linker based LMOFs having potential to detect organic pollutants *viz.*, nitroaromatics, acetone, acetylacetone, and paraquat as well as inorganic pollutants including di- and trivalent metal cations *viz*, Hg^{2+}, Cu^{2+}, Pb^{2+}, Pd^{2+}, Al^{3+}, Fe^{3+} and Cr^{3+}; and inorganic anions such as cyanide, iodide, chromate, dichromate and manganate anions in aqueous medium. The origin of fluorescence in LMOFs comprising Zn(II)/Cd(II) and mixed linkers and their aquatic stability is also discussed. It has been seen that the Zn(II)/Cd(II) and mixed linker based LMOF offer advantages such as aquatic stability and also a rapid, selective, and sensitive response towards the analyte. The selectivity of LMOF/LCP based chemosensors may be attributed to the intricate surface and pore geometries of the framework. This also justifies the scarcity of MOF based sensors for very small ions such as fluoride as well as very large biomolecules, *viz.*, DNA, and enzymes. With the pace at which the concerned research field is developing, it is fairly logical to anticipate Zn(II)/Cd(II) and mixed linker based LMOFs/LCPs for selective and sensitive fluorosensing of biomaterials in the coming times.

Conflicts of interest

There are no conflicts to declare.

Acknowledgements

The registration number of this publication is the CSIR-CSMCRI – 158/2019. Financial support from CSIR-SRF (BP) is gratefully acknowledged.

References

1 Z. Hu, B. J. Deibert and J. Li, Luminescent metal–organic frameworks for chemical sensing and explosive detection, *Chem. Soc. Rev.*, 2014, **43**, 5815–5840.
2 Y. Zhang, S. Yuan, G. Day, X. Wang, X. Yang and H.-C. Zhou, Luminescent sensors based on metal-organic frameworks, *Coord. Chem. Rev.*, 2018, **354**, 28–45.
3 P. Samanta, A. V. Desai, Su. Let and S. K. Ghosh, Advanced Porous Materials for Sensing, Capture and Detoxification of Organic Pollutants toward Water Remediation, *ACS Sustainable Chem. Eng.*, 2019, **7**, 7456–7478.

4 Q. Gao, J. Xu and X.-H. Bu, Recent advances about metal–organic frameworks in the removal of pollutants from wastewater, *Coord. Chem. Rev.*, 2019, **378**, 17–31.
5 L. M. Kustov, V. I. Isaeva, J. Přech and K. K. Bisht, Metal-organic frameworks as materials for applications in sensors, *Mendeleev Commun.*, 2019, **29**, 361–368.
6 P. Devi, P. Singh and S. K. Kansal, *Inorganic Pollutants in Water*, Elsevier, 1st edn, 2020, ISBN: 9780128189658.
7 S. Chatterjee and A. R. Paital, Functionalized Cubic Mesoporous Silica as a Non-Chemodosimetric Fluorescence Probe and Adsorbent for Selective Detection and Removal of Bisulfite Anions along with Toxic Metal Ions, *Adv. Funct. Mater.*, 2017, **28**, 1704726.
8 S. Bhatt, M. Bhatt, A. Kumar, G. Vyas, T. Gajaria and P. Paul, Green route for synthesis of multifunctional fluorescent carbon dots from Tulsi leaves and its application as Cr(VI) sensors, bio-imaging and patterning agents, *Colloids Surf., B*, 2018, **167**, 126–133.
9 L. F. Kreno, K. Leong, O. K. Farha, M. Allendorf, R. P. Van Duyne and J. T. Hupp, Metal–Organic Framework Materials as Chemical Sensors, *Chem. Rev.*, 2012, **112**, 1105–1125.
10 G. Vyas, S. Bhatt and P. Paul, Synthesis of Calixarene-Capped Silver Nanoparticles for Colorimetric and Amperometric Detection of Mercury (Hg^{II}, Hg^{0}), *ACS Omega*, 2019, **4**, 3860–3870.
11 Y. Wang, A. La, Y. Ding, Y. Liu and Y. Lei, Novel Signal-Amplifying Fluorescent Nanofibers for Naked-Eye-Based Ultrasensitive Detection of Buried Explosives and Explosive Vapors, *Adv. Funct. Mater.*, 2012, **22**, 3547–3555.
12 S. Chatterjee, H. Gohil, I. Raval, S. Chatterjee and A. R. Paital, An Anthracene Excimer Fluorescence Probe on Mesoporous Silica for Dual Functions of Detection and Adsorption of Mercury(II) and Copper(II) with Biological In Vivo Applications, *Small*, 2019, **15**, 1804749.
13 S. Rochat and T. M. Swager, Conjugated Amplifying Polymers for Optical Sensing Applications, *ACS Appl. Mater. Interfaces*, 2013, **5**, 4488–4502.
14 A. H. Malik, S. Hussain, A. Kalita and P. K. Iyer, Conjugated Polymer Nanoparticles for the Amplified Detection of Nitro-explosive Picric Acid on Multiple Platforms, *ACS Appl. Mater. Interfaces*, 2015, **7**, 26968–26976.
15 D. Banerjee, Z. Hu and J. Li, Luminescent metal–organic frameworks as explosive sensors, *Dalton Trans.*, 2014, **43**, 10668–10685.
16 S. S. Nagarkar, A. V. Desai and S. K. Ghosh, Engineering metal–organic frameworks for aqueous phase 2,4,6-trinitrophenol (TNP) sensing, *CrystEngComm*, 2016, **18**, 2994–3007.
17 F.-Y. Yi, D. Chen, M.-K. Wu, L. Han and H.-L. Jiang, Chemical Sensors Based on Metal–Organic Frameworks, *ChemPlusChem*, 2016, **81**, 675–690.
18 W. P. Lustig, S. Mukherjee, N. D. Rudd, A. V. Desai, J. Li and S. K. Ghosh, Metal–organic frameworks: functional luminescent and photonic materials for sensing applications, *Chem. Soc. Rev.*, 2017, **46**, 3242–3285.
19 B. Yan, Lanthanide-Functionalized Metal–Organic Framework Hybrid Systems To Create Multiple Luminescent Centers for Chemical Sensing, *Acc. Chem. Res.*, 2017, **50**, 2789–2798.
20 J. Dong, D. Zhao, Y. Lu and W.-Y. Sun, Photoluminescent metal–organic frameworks and their application for sensing biomolecules, *J. Mater. Chem. A*, 2019, **7**, 22744–22767.
21 X.-D. Zhang, Y. Zhao, K. Chen, P. Wang, Y.-S. Kang, H. Wu and W.-Y. Sun, Cucurbit[6]uril-based multifunctional supramolecular assemblies: synthesis, removal of Ba(II) and fluorescence sensing of Fe(III), *Dalton Trans.*, 2018, **47**, 3958–3964.
22 N. C. Burtch, H. Jasuja and K. S. Walton, Water Stability and Adsorption in Metal–Organic Frameworks, *Chem. Rev.*, 2014, **114**, 10575–10612.
23 J. Canivet, A. Fateeva, Y. Guo, B. Coasne and D. Farrusseng, Water adsorption in MOFs: fundamentals and applications, *Chem. Soc. Rev.*, 2014, **43**, 5594–5617.
24 M. D. Allendorf, C. A. Bauer, R. K. Bhakta and R. J. T. Houk, Luminescent metal–organic frameworks, *Chem. Soc. Rev.*, 2009, **38**, 1330–1352.
25 Y. Cui, Y. Yue, G. Qian and B. Chen, Luminescent Functional Metal–Organic Frameworks, *Chem. Rev.*, 2012, **112**, 1126–1162.
26 L. Chen, D. Liu, J. Peng, Q. Du and H. He, Ratiometric fluorescence sensing of metal-organic frameworks: Tactics and perspectives, *Coord. Chem. Rev.*, 2020, **404**, 213113.
27 N. B. Shustova, B. D. McCarthy and M. Dinca, Turn-On Fluorescence in Tetraphenylethylene-Based Metal–Organic Frameworks: An Alternative to Aggregation-Induced Emission, *J. Am. Chem. Soc.*, 2011, **133**, 20126–20129.
28 J. Yu, Y. Cui, H. Xu, Y. Yang, Z. Wang, B. Chen and G. Qian, Confinement of pyridinium hemicyanine dye within an anionic metal-organic framework for two-photon-pumped lasing, *Nat. Commun.*, 2013, **4**, 2719.
29 S. Bordiga, C. Lamberti, G. Ricchiardi, L. Regli, F. Bonino, A. Damin, K.-P. Lillerud, M. Bjorgenb and A. Zecchina, Electronic and vibrational properties of a MOF-5 metal–organic framework: ZnO quantum dot behaviour, *Chem. Commun.*, 2004, 2300–2301.
30 C. A. Bauer, T. V. Timofeeva, T. B. Settersten, B. D. Patterson, V. H. Liu, B. A. Simmons and M. D. Allendorf, Influence of Connectivity and Porosity on Ligand-Based Luminescence in Zinc Metal–Organic Frameworks, *J. Am. Chem. Soc.*, 2007, **129**, 7136–7144.
31 J.-G. Lin, Y.-Y. Xu, L. Qiu, S.-Q. Zang, C.-S. Lu, C.-Y. Duan, Y.-Z. Li, S. Gao and Q.-J. Meng, Ligand-to-metal ratio controlled assembly of nanoporous metal–organic frameworks, *Chem. Commun.*, 2008, 2659–2661.
32 S. Y. Zhua and B. Yan, A novel covalent post-synthetically modified MOF hybrid as a sensitive and selective fluorescent probe for Al^{3+} detection in aqueous media, *Dalton Trans.*, 2018, **47**, 1674–1681.
33 S. Sharma and S. K. Ghosh, Metal–Organic Framework-Based Selective Sensing of Biothiols via Chemidosimetric Approach in Water, *ACS Omega*, 2018, **3**, 254–258.

34 J.-C. Dai, X.-T. Wu, Z.-Y. Fu, S.-M. Hu, W.-X. Du, C.-P. Cui, L.-M. Wu, H.-H. Zhang and R.-Q. Sun, Synthesis, Structure, and Fluorescence of the Novel Cadmium(II)–Trimesate Coordination Polymers with Different Coordination Architectures, *Inorg. Chem.*, 2002, **41**, 1391–1396.

35 W. Chen, J.-Y. Wang, C. Chen, Q. Yue, H.-M. Yuan, J.-S. Chen and S.-N. Wang, Photoluminescent Metal–Organic Polymer Constructed from Trimetallic Clusters and Mixed Carboxylates, *Inorg. Chem.*, 2003, **42**, 944–946.

36 K. K. Bisht, A. C. Kathalikkattil and E. Suresh, Structure modulation, argentophilic interactions and photoluminescence properties of silver(I) coordination polymers with isomeric N-donor ligands, *RSC Adv.*, 2012, **2**, 8421–8428.

37 M. Zhang, L. Zhang, Z. Xiao, Q. Zhang, R. Wang, F. Dai and D. Sun, Pentiptycene-Based Luminescent Cu(II) MOF Exhibiting Selective Gas Adsorption and Unprecedentedly High-Sensitivity Detection of Nitroaromatic Compounds (NACs), *Sci. Rep.*, 2016, **6**, 20672.

38 E. A. Dolgopolova, O. A. Ejegbavwo, C. R. Martin, M. D. Smith, W. Setyawan, S. G. Karakalos, C. H. Henager, H. C. Zur Loye and N. B. Shustova, Multifaceted Modularity: A Key for Stepwise Building of Hierarchical Complexity in Actinide Metal–Organic Frameworks, *J. Am. Chem. Soc.*, 2017, **139**, 16852–16861.

39 S. Khatua, S. Goswami, S. Biswas, K. Tomar, H. S. Jena and S. Konar, Stable Multiresponsive Luminescent MOF for Colorimetric Detection of Small Molecules in Selective and Reversible Manner, *Chem. Mater.*, 2015, **27**, 5349–5360.

40 G. Lu and J. T. Hupp, Metal–Organic Frameworks as Sensors: A ZIF-8 Based Fabry–Pérot Device as a Selective Sensor for Chemical Vapors and Gases, *J. Am. Chem. Soc.*, 2010, **132**, 7832–7833.

41 J. D. Einkauf, T. T. Kelley, B. C. Chan and D. T. de Lill, Rethinking Sensitized Luminescence in Lanthanide Coordination Polymers and MOFs: Band Sensitization and Water Enhanced Eu Luminescence in $[Ln(C_{15}H_9O_5)_3(H_2O)_3]_n$ (Ln = Eu, Tb), *Inorg. Chem.*, 2016, **55**, 7920–7927.

42 P. Chandrasekhar, A. Mukhopadhyay, G. Savitha and J. N. Moorthy, Remarkably selective and enantiodifferentiating sensing of histidine by a fluorescent homochiral Zn-MOF based on pyrene-tetralactic acid, *Chem. Sci.*, 2016, **7**, 3085–3091.

43 B. Manna, A. V. Desai and S. K. Ghosh, Neutral N-donor ligand based flexible metal–organic frameworks, *Dalton Trans.*, 2016, **45**, 4060–4072.

44 B. Chen, Y. Yang, F. Zapata, G. Lin, G. Qian and E. B. Lobkovsky, Luminescent Open Metal Sites within a Metal–Organic Framework for Sensing Small Molecules, *Adv. Mater.*, 2007, **19**, 1693–1696.

45 D. Tanaka, S. Horike, S. Kitagawa, M. Ohba, M. Hasegawa, Y. Ozawa and K. Toriumi, Anthracene array-type porous coordination polymer with host–guest charge transfer interactions in excited states, *Chem. Commun.*, 2007, 3142–3144.

46 C. Serre, F. Pelle, N. Gardant and G. Ferey, Synthesis and Characterization of MIL†-79 and MIL-80: Two New Luminescent Open-Framework Rare-Earth Dicarboxylates with Unusual 1D Inorganic Subnetworks, *Chem. Mater.*, 2004, **16**, 1177–1182.

47 S. S. Nagarkar, B. Joarder, A. K. Chaudhari, S. Mukherjee and S. K. Ghosh, Highly Selective Detection of Nitro Explosives by a Luminescent Metal–Organic Framework, *Angew. Chem., Int. Ed.*, 2013, **52**, 2881–2885.

48 Y.-N. Gong, L. Jiang and T.-B. Lu, A highly stable dynamic fluorescent metal–organic framework for selective sensing of nitroaromatic explosives, *Chem. Commun.*, 2013, **49**, 11113–11115.

49 S.-R. Zhang, D.-Y. Du, J.-S. Qin, S.-J. Bao, S.-L. Li, W.-W. He, Y.-Q. Lan, P. Shen and Z.-M. Su, A Fluorescent Sensor for Highly Selective Detection of Nitroaromatic Explosives Based on a 2D, Extremely Stable, Metal–Organic Framework, *Chem. – Eur. J.*, 2014, **20**, 3589–3594.

50 I.-H. Park, R. Medishetty, J.-Y. Kim, S. S. Lee and J. J. Vittal, Distortional Supramolecular Isomers of Polyrotaxane Coordination Polymers: Photoreactivity and Sensing of Nitro Compounds, *Angew. Chem., Int. Ed.*, 2014, **53**, 5591–5595.

51 D. Ma, B. Li, X. Zhou, Q. Zhou, K. Liu, G. Zeng, G. Li, Z. Shi and S. Feng, A dual functional MOF as a luminescent sensor for quantitatively detecting the concentration of nitrobenzene and temperature, *Chem. Commun.*, 2013, **49**, 8964–8966.

52 B. Gole, A. K. Bar and P. S. Mukherjee, Multicomponent Assembly of Fluorescent-Tag Functionalized Ligands in Metal–Organic Frameworks for Sensing Explosives, *Chem. – Eur. J.*, 2014, **20**, 13321–13336.

53 Y.-S. Xue, Y. He, L. Zhou, F.-J. Chen, Y. Xu, H.-B. Du, X.-Z. You and B. Chen, A photoluminescent microporous metal organic anionic framework for nitroaromatic explosive sensing, *J. Mater. Chem. A*, 2013, **1**, 4525–4530.

54 Y. Rachuri, B. Parmar, K. K. Bisht and E. Suresh, Structural studies and detection of nitroaromatics by luminescent 2D coordination polymers with angular dicarboxylate ligands, *Inorg. Chem. Front.*, 2015, **2**, 228–236.

55 P. Küsgens, M. Rose, I. Senkovska, H. Fröde, A. Henschel, S. Siegle and S. Kaskel, Characterization of metal-organic frameworks by water adsorption, *Microporous Mesoporous Mater.*, 2009, **120**, 325–330.

56 K. A. Cychosz and A. J. Matzger, Water Stability of Microporous Coordination Polymers and the Adsorption of Pharmaceuticals from Water, *Langmuir*, 2010, **26**, 17198–17202.

57 A. J. Lan, K. H. Li, H. H. Wu, D. H. Olson, T. J. Emge, W. Ki, M. C. Hong and J. Li, A Luminescent Microporous Metal–Organic Framework for the Fast and Reversible

Detection of High Explosives, *Angew. Chem., Int. Ed.*, 2009, **48**, 2334–2338.

58 S. Pramanik, C. Zheng, X. Zhang, T. J. Emge and J. Li, New Microporous Metal–Organic Framework Demonstrating Unique Selectivity for Detection of High Explosives and Aromatic Compounds, *J. Am. Chem. Soc.*, 2011, **133**, 4153–4155.

59 Y. Li, H. Song, Q. Chen, K. Liu, F. Y. Zhao, W. J. Ruan and Z. Chang, Two coordination polymers with enhanced ligand-centered luminescence and assembly imparted sensing ability for acetone, *J. Mater. Chem. A*, 2014, **2**, 9469–9473.

60 Y. Rachuri, B. Parmar, J. F. Kurisingal, K. K. Bisht, D.-W. Park and E. Suresh, Metal Organic Frameworks for Detection of Organic Nitro Compounds, *Metal Organic Frameworks*, ed. V. Mittal, Central West Publishing, 2019, pp. 187–237, ISBN: 9781925823578.

61 X.-D. Zhang, Y. Zhao, K. Chen, J.-H. Guo, P. Wang, H. Wu and W.-Y. Sun, Cucurbit[6]uril-based supramolecular assemblies incorporating metal complexes with multiaromatic ligands as structure-directing agent for detection of aromatic amines and nitroaromatic compounds, *Sens. Actuators, B*, 2019, **282**, 844–853.

62 R. Benigni and L. Passerini, Carcinogenicity of the aromatic amines: from structure–activity relationships to mechanisms of action and risk assessment, *Mutat. Res.*, 2002, **511**, 191–206.

63 C.-L. Tao, B. Chen, X.-G. Liu, L.-J. Zhou, X.-L. Zhu, J. Cao, Z.-G. Gu, Z. Zhao, L. Shen and B. Z. Tang, A highly luminescent entangled metal–organic framework based on pyridine-substituted tetraphenylethene for efficient pesticide detection, *Chem. Commun.*, 2017, **53**, 9975–9978.

64 B. Joarder, A. V. Desai, P. Samanta, S. Mukherjee and S. K. Ghosh, Selective and Sensitive Aqueous-Phase Detection of 2,4,6-Trinitrophenol (TNP) by an Amine-Functionalized Metal–Organic Framework, *Chem. – Eur. J.*, 2015, **21**, 965–969.

65 M.-M. Chen, X. Zhou, H.-X. Li, X.-X. Yang and J.-P. Lang, Luminescent Two-Dimensional Coordination Polymer for Selective and Recyclable Sensing of Nitroaromatic Compounds with High Sensitivity in Water, *Cryst. Growth Des.*, 2015, **15**, 2753–2760.

66 S. Mukherjee, A. V. Desai, B. Manna, A. I. Inamdar and S. K. Ghosh, Exploitation of Guest Accessible Aliphatic Amine Functionality of a Metal–Organic Framework for Selective Detection of 2,4,6-Trinitrophenol (TNP) in Water, *Cryst. Growth Des.*, 2015, **15**, 4627–4634.

67 B.-Q. Song, C. Qin, Y.-T. Zhang, X.-S. Wu, L. Yang, K.-Z. Shao and Z.-M. Su, Spontaneous chiral resolution of a rare 3D self-penetration coordination polymer for sensitive aqueous-phase detection of picric acid, *Dalton Trans.*, 2015, **44**, 18386–18394.

68 Y.-J. Yang, M.-J. Wang and K.-L. Zhang, A novel photoluminescent Cd(II)–organic framework exhibiting rapid and efficient multi-responsive fluorescence sensing for trace amounts of Fe^{3+} ions and some NACs, especially for 4-nitroaniline and 2-methyl-4-nitroaniline, *J. Mater. Chem. C*, 2016, **4**, 11404–11418.

69 B. Parmar, Y. Rachuri, K. K. Bisht and E. Suresh, Syntheses and Structural Analyses of New 3D Isostructural Zn(II) and Cd(II) Luminescent MOFs and their Application Towards Detection of Nitroaromatics in Aqueous Media, *ChemistrySelect*, 2016, **1**, 6308–6315.

70 Y. Rachuri, B. Parmar, K. K. Bisht and E. Suresh, Mixed ligand two dimensional Cd(II)/Ni(II) metal organic frameworks containing dicarboxylate and tripodal N-donor ligands: Cd(II) MOF is an efficient luminescent sensor for detection of picric acid in aqueous media, *Dalton Trans.*, 2016, **45**, 7881–7892.

71 X.-J. Liu, Y.-H. Zhang, Z. Chang, A.-L. Li, D. Tian, Z.-Q. Yao, Y.-Y. Jia and X.-H. Bu, A Water-Stable Metal–Organic Framework with a Double-Helical Structure for Fluorescent Sensing, *Inorg. Chem.*, 2016, **55**, 7326–7328.

72 S. Senthilkumar, R. Goswami, N. L. Obasi and S. Neogi, Construction of Pillar-Layer Metal–Organic Frameworks for CO_2 Adsorption under Humid Climate: High Selectivity and Sensitive Detection of Picric Acid in Water, *ACS Sustainable Chem. Eng.*, 2017, **5**, 11307–11315.

73 Y. Deng, N. Chen, Q. Li, X. Wu, X. Huang, Z. Lin and Y. Zhao, Systematic Study of Mutually Inclusive Influences of Temperature and Substitution on the Coordination Geometry of Co(II) in a Series of Coordination Polymers and Their Properties, *Cryst. Growth Des.*, 2017, **17**, 3170–3179.

74 Y. Rachuri, B. Parmar, K. K. Bisht and E. Suresh, Multiresponsive Adenine-Based Luminescent Zn(II) Coordination Polymer for Detection of Hg^{2+} and Trinitrophenol in Aqueous Media, *Cryst. Growth Des.*, 2017, **17**, 1363–1372.

75 V. Sharma, D. De, S. Pal, P. Saha and P. K. Bharadwaj, A 2D Coordination Network That Detects Nitro Explosives in Water, Catalyzes Baylis–Hillman Reactions, and Undergoes Unusual 2D→D Single-Crystal to Single-Crystal Transformation, *Inorg. Chem.*, 2017, **56**, 8847–8855.

76 G. Chakraborty and S. K. Mandal, Neutral Luminescent Metal-Organic Frameworks: Structural Diversification, Photophysical Properties, and Sensing Applications, *Inorg. Chem.*, 2017, **56**, 14556–14566.

77 B. Parmar, Y. Rachuri, K. K. Bisht, R. Laiya and E. Suresh, Mechanochemical and Conventional Synthesis of Zn(II)/Cd(II) Luminescent Coordination Polymers: Dual Sensing Probe for Selective Detection of Chromate Anions and TNP in Aqueous Phase, *Inorg. Chem.*, 2017, **56**, 2627–2638.

78 G. Chakraborty, P. Das and S. K. Mandal, Strategic Construction of Highly Stable Metal–Organic Frameworks Combining Both Semi-Rigid Tetrapodal and Rigid Ditopic Linkers: Selective and Ultrafast Sensing of 4-Nitroaniline in Water, *ACS Appl. Mater. Interfaces*, 2018, **10**, 42406–42416.

79 D. Das and K. Biradha, Luminescent Coordination Polymers of Naphthalene Based Diamide with Rigid and

Flexible Dicarboxylates: Sensing of Nitro Explosives, Fe(III) Ion, and Dyes, *Cryst. Growth Des.*, 2018, **18**, 3683–3692.

80 Z.-W. Zhai, S.-H. Yang, M. Cao, L.-K. Li, C.-X. Du and S.-Q. Zang, Rational Design of Three Two-Fold Interpenetrated Metal–Organic Frameworks: Luminescent Zn/Cd-Metal–Organic Frameworks for Detection of 2,4,6-Trinitrophenol and Nitrofurazone in the Aqueous Phase, *Cryst. Growth Des.*, 2018, **18**, 7173–7182.

81 Y. Rachuri, B. Parmar and E. Suresh, Three-Dimensional Co(II)/Cd(II) Metal–Organic Frameworks: Luminescent Cd-MOF for Detection and Adsorption of 2,4,6-Trinitrophenol in the Aqueous Phase, *Cryst. Growth Des.*, 2018, **18**, 3062–3072.

82 Z. Zhou, M.-L. Han, H.-R. Fu, L.-F. Ma, F. Luo and D.-S. Li, Engineering design toward exploring the functional group substitution in 1D channels of Zn–organic frameworks upon nitro explosives and antibiotics detection, *Dalton Trans.*, 2018, **47**, 5359–5365.

83 Y. Wu, Z. Gu, W. Luo, L. Wu, Y. Li, B. Xie and L. Zou, Crystal structure, luminescent sensing and photocatalytic activity of a multifunctional hydrazone-based zinc(II) coordination polymer, *Transition Met. Chem.*, 2018, **43**, 673–581.

84 H. Jin, J. Xu, L. Zhang, B. Ma, X. Shi, Y. Fan and L. Wang, Multi-responsive luminescent sensor based on Zn(II) metal-organic framework for selective sensing of Cr(III), Cr(VI) ions and p-nitrotolune, *J. Solid State Chem.*, 2018, **268**, 168–174.

85 X. Wang, Y. Han, X. X. Han, X. Hou, J.-J. Wang and F. Fu, Highly selective and sensitive detection of Hg^{2+}, $Cr_2O_7^{2-}$, and nitrobenzene/2,4-dinitrophenol in water via two fluorescent Cd-CPs, *New J. Chem.*, 2018, **42**, 19844–19852.

86 G. Chakraborty, P. Das and S. K. Mandal, Structural Diversity in Luminescent MOFs Containing a Bent Electron-rich Dicarboxylate Linker and a Flexible Capping Ligand: Selective Detection of 4-Nitroaniline in Water, *Chem. – Asian J.*, 2019, **14**, 3712–3720.

87 A. Gogia and S. K. Mandal, A rational design and green synthesis of 3D metal organic frameworks containing a rigid heterocyclic nitrogen-rich dicarboxylate: structural diversity, CO_2 sorption and selective sensing of 2,4,6-TNP in water, *Dalton Trans.*, 2019, **48**, 2388–2398.

88 T. Kumar, M. Venkateswarulu, B. Das, A. Halder and R. R. Koner, Zn(II)-based coordination polymer: An emissive signaling platform for the recognition of an explosive and a pesticide in an aqueous system, *Dalton Trans.*, 2019, **48**, 12382–12385.

89 X.-M. Kang, X.-Y. Fan, P.-Y. Hao, W.-M. Wang and B. Zhao, A stable zinc–organic framework with luminescence detection of acetylacetone in aqueous solution, *Inorg. Chem. Front.*, 2019, **6**, 271–277.

90 S. S. Dhankhar, N. Sharma and C. M. Nagaraja, Construction of bifunctional 2-fold interpenetrated Zn(II) MOFs exhibiting selective CO_2 adsorption and aqueous-phase sensing of 2,4,6-trinitrophenol, *Inorg. Chem. Front.*, 2019, **6**, 1058–1067.

91 H. Chen, P. Fan, X. Tu, H. Min, X. Yu, X. Li, J.-L. Zeng, S. Zhang and P. Cheng, A Bifunctional Luminescent Metal–Organic Framework for the Sensing of Paraquat and Fe^{3+} Ions in Water, *Chem. – Asian J.*, 2019, **14**, 3611–3619.

92 X. Zhang, H. Chen, B. Li, G. Liu and X. Liu, Construction of functional coordination polymers derived from designed flexible bis(4-carboxybenzyl)amine, *CrystEngComm*, 2019, **21**, 1231–1241.

93 C. Xu, C. Bi, Z. Zhu, R. Luo, X. Zhang, D. Zhang, C. Fan, L. Cui and Y. Fan, Metal–organic frameworks with 5,5′-(1,4-xylylenediamino) diisophthalic acid and various nitrogen-containing ligands for selectively sensing Fe(III)/Cr(VI) and nitroaromatic compounds, *CrystEngComm*, 2019, **21**, 2333–2344.

94 M. Zhang, Y. Zheng, M. Liu, Y. Ren, Z. Wang, J. Cao and J. Wang, Two zinc(II) coordination polymers based on flexible co-ligands featuring assembly imparted sensing abilities for $Cr_2O_7^{2-}$ and *o*-NP, *RSC Adv.*, 2019, **9**, 21086–21094.

95 T. Wiwasuku, J. Boonmak, K. Siriwong, V. Ervithayasuporn and S. Youngme, Highly sensitive and selective fluorescent sensor based on a multi-responsive ultrastable amino-functionalized Zn(II)-MOF for hazardous chemicals, *Sens. Actuators, B*, 2019, **284**, 403–413.

96 X. Zhuang, X. Zhang, N. Zhang, Y. Wang, L. Zhao and Q. Yang, Novel Multifunctional Zn Metal–Organic Framework Fluorescent Probe Demonstrating Unique Sensitivity and Selectivity for Detection of PA and Fe^{3+} Ions in Water Solution, *Cryst. Growth Des.*, 2019, **19**, 5729–5736.

97 J. Zhang, W. Jia, J. Wu, G. Tang and C. Zhang, Two mixed-ligand Cd(II)–organic frameworks with unique topologies: selective luminescence sensing of TNP and Cu^{2+} ions with recyclable performances, *New J. Chem.*, 2019, **43**, 16078–16088.

98 R. M. Duke, E. B. Veale, F. M. Pfeffer, P. E. Kruger and T. Gunnlaugsson, Colorimetric and fluorescent anion sensors: an overview of recent developments in the use of 1,8-naphthalimide-based chemosensors, *Chem. Soc. Rev.*, 2010, **39**, 3936–3953.

99 H. T. Ngo, X. Liu and K. A. Jolliffe, Anion recognition and sensing with Zn(II)–dipicolylamine complexes, *Chem. Soc. Rev.*, 2012, **41**, 4928–4965.

100 F. C. R. Manning, L. J. Blankenship, J. P. Wise, J. Xu, L. C. Bridgewater and S. R. Patierno, Induction of Internucleosomal DNA Fragmentation by Carcinogenic Chromate: Relationship to DNA Damage, Genotoxicity, and Inhibition of Macromolecular Synthesis, *Environ. Health Perspect.*, 1994, **102**, 159–167.

101 C. M. Thompson, C. R. Kirman, D. M. Proctor, L. C. Haws, M. Suh, S. M. Hays, J. G. Hixon and M. A. Harris, A chronic oral reference dose for hexavalent chromium-induced intestinal cancer, *J. Appl. Toxicol.*, 2014, **34**, 525–536.

102 A. Zhitkovich, Importance of Chromium–DNA Adducts in Mutagenicity and Toxicity of Chromium(VI), *Chem. Res. Toxicol.*, 2005, **18**, 3–11.

103 K. P. Carter, A. M. Young and A. E. Palmer, Fluorescent Sensors for Measuring Metal Ions in Living Systems, *Chem. Rev.*, 2014, **114**, 4564–4601.
104 X. F. Liu and E. C. Theil, Ferritins: Dynamic Management of Biological Iron and Oxygen Chemistry, *Acc. Chem. Res.*, 2005, **38**, 167–175.
105 F. Cai, Q. Wang, X. Chen, W. Qiu, F. Zhan, F. Gao and Q. Wang, Selective binding of Pb^{2+} with manganese-terephthalic acid MOF/SWCNTs: Theoretical modeling, experimental study and electroanalytical application, *Biosens. Bioelectron.*, 2017, **98**, 310–316.
106 B. Wang, W. Xing, Y. Zhao and X. Deng, Effects of chronic aluminum exposure on memory through multiple signal transduction pathways, *Environ. Toxicol. Pharmacol.*, 2010, **29**, 308–313.
107 E. Altschuler, Aluminum-Containing Antacids as a Cause of Idiopathic Parkinson's Disease, *Med. Hypotheses*, 1999, **53**, 22–23.
108 F.-Y. Yi, J.-P. Li, D. Wu and Z.-M. Sun, A Series of Multifunctional Metal–Organic Frameworks Showing Excellent Luminescent Sensing, Sensitization, and Adsorbent Abilities, *Chem. – Eur. J.*, 2015, **21**, 11475–11482.
109 F.-L. Hu, Y.-X. Shi, H.-H. Chen and J.-P. Lang, A Zn(II) coordination polymer and its photocycloaddition product: syntheses, structures, selective luminescence sensing of iron(III) ions and selective absorption of dyes, *Dalton Trans.*, 2015, **44**, 18795–18803.
110 L. Wen, X. Zheng, K. Lv, C. Wang and X. Xu, Two Amino-Decorated Metal–Organic Frameworks for Highly Selective and Quantitatively Sensing of Hg^{II} and Cr^{VI} in Aqueous Solution, *Inorg. Chem.*, 2015, **54**, 7133–7135.
111 B.-L. Hou, D. Tian, J. Liu, L.-Z. Dong, S.-L. Li, D.-S. Li and Y.-Q. Lan, A Water-Stable Metal–Organic Framework for Highly Sensitive and Selective Sensing of Fe^{3+} Ion, *Inorg. Chem.*, 2016, **55**, 10580–10586.
112 Y. Zhao, X. Xu, L. Qiu, X. Kang, L. Wen and B. Zhang, Metal–Organic Frameworks Constructed from a New Thiophene-Functionalized Dicarboxylate: Luminescence Sensing and Pesticide Removal, *ACS Appl. Mater. Interfaces*, 2017, **9**, 15164–15175.
113 A. Karmakar, B. Joarder, A. Mallick, P. Samanta, A. V. Desai, S. Basu and S. K. Ghosh, Aqueous phase sensing of cyanide ions using a hydrolytically stable metal–organic framework, *Chem. Commun.*, 2017, **53**, 1253–1256.
114 J. Zhang, J. Wu, L. Gong, J. Feng and C. Zhang, Water-Stable Luminescent Zn(II) Metal-Organic Framework as Rare Multifunctional Sensor for Cr(VI) and TNP, *ChemistrySelect*, 2017, **2**, 7465–7473.
115 S. Chen, Z. Shi, L. Qin, H. Jia and H. Zheng, Two New Luminescent Cd(II)-Metal–Organic Frameworks as Bifunctional Chemosensors for Detection of Cations Fe^{3+}, Anions $CrO4^{2-}$, and $Cr_2O_7^{2-}$ in Aqueous Solution, *Cryst. Growth Des.*, 2017, **17**, 67–72.
116 W.-J. Gong, R. Yao, H.-X. Li, Z.-G. Ren, J.-G. Zhang and J.-P. Lang, Luminescent cadmium(II) coordination polymers of 1,2,4,5-tetrakis(4-pyridylvinyl)benzene used as efficient multi-responsive sensors for toxic metal ions in water, *Dalton Trans.*, 2017, **46**, 16861–16871.
117 X.-X. Jia, R.-X. Yao, F.-Q. Zhang and X.-M. Zhang, A Fluorescent Anionic MOF with $Zn_4(trz)_2$ Chain for Highly Selective Visual Sensing of Contaminants: Cr(III) Ion and TNP, *Inorg. Chem.*, 2017, **56**, 2690–2696.
118 T.-Y. Gu, M. Dai, D. J. Young, Z.-G. Ren and J.-P. Lang, Luminescent Zn(II) Coordination Polymers for Highly Selective Sensing of Cr(III) and Cr(VI) in Water, *Inorg. Chem.*, 2017, **56**, 4668–4678.
119 S. A. A. Razavi, M. Y. Masoomi and A. Morsali, Double Solvent Sensing Method for Improving Sensitivity and Accuracy of Hg(II) Detection Based on Different Signal Transduction of a Tetrazine-Functionalized Pillared Metal–Organic Framework, *Inorg. Chem.*, 2017, **56**, 9646–9652.
120 B. Parmar, Y. Rachuri, K. K. Bisht and E. Suresh, Mixed-Ligand LMOF Fluorosensors for Detection of Cr(VI) Oxyanions and Fe^{3+}/Pd^{2+} Cations in Aqueous Media, *Inorg. Chem.*, 2017, **56**, 10939–10949.
121 Y. Lin, X. Zhang, W. Chen, W. Shi and P. Cheng, Three Cadmium Coordination Polymers with Carboxylate and Pyridine Mixed Ligands: Luminescent Sensors for Fe^{III} and Cr^{VI} Ions in an Aqueous Medium, *Inorg. Chem.*, 2017, **56**, 11768–11778.
122 J. Zhang, L. Gong, J. Feng, J. Wu and C. Zhang, Two luminescent Zn(II)/Cd(II) metal–organic frameworks as rare multifunctional sensors, *New J. Chem.*, 2017, **41**, 8107–8117.
123 X.-M. Meng, X. Zhang, P.-F. Qi, Z.-A. Zong, F. Jin and Y.-H. Fan, Syntheses, structures, luminescent and photocatalytic properties of various polymers based on a "V"-shaped dicarboxylic acid, *RSC Adv.*, 2017, **7**, 4855–4871.
124 Q. Li, X. Wu, X. Huang, Y. Deng, N. Chen, D. Jiang, L. Zhao, Z. Lin and Y. Zhao, Tailoring the Fluorescence of AIE-Active Metal–Organic Frameworks for Aqueous Sensing of Metal Ions, *ACS Appl. Mater. Interfaces*, 2018, **10**, 3801–3809.
125 L. Fan, Y. Zhang, J. Liang, X. Wang, H. Lv, J. Wang, L. Zhao and X. Zhang, Structural diversity, magnetic properties, and luminescence sensing of five 3D coordination polymers derived from designed 3,5-di(2′,4′-dicarboxylphenyl)benozoic acid, *CrystEngComm*, 2018, **20**, 4752–4762.
126 Z.-J. Wang, L.-J. Han, X.-J. Gao and H.-G. Zheng, Three Cd(II) MOFs with Different Functional Groups: Selective CO_2 Capture and Metal Ions Detection, *Inorg. Chem.*, 2018, **57**, 5232–5239.
127 D. K. Singha, P. Majee, S. K. Mondal and P. Mahata, A luminescent cadmium based MOF as selective and sensitive iodide sensor in aqueous medium, *J. Photochem. Photobiol., A*, 2018, **356**, 389–396.
128 M.-N. Zhang, T.-T. Fan, Q.-S. Wang, H.-L. Han and X. Li, Zn/Cd/Cu- frameworks constructed by 3,3′-diphenyldicarboxylate and 1,4-bis(1,2,4-triazol-1-yl)butane: Syntheses,

structure, luminescence and luminescence sensing for metal ion in aqueous medium, *J. Solid State Chem.*, 2018, **258**, 744–752.

129 X.-X. Zhao, Z.-B. Qin, Y.-H. Li and G.-H. Cui, New Cd(II) and Zn(II) coordination polymers showing luminescent sensing for Fe(III) and photocatalytic degrading methylene blue, *Polyhedron*, 2018, **153**, 197–204.

130 Y.-Q. Zhang, V. A. Blatov, X.-X. Lv, C.-H. Yang, L.-L. Qian, K. Li, B.-L. Li and B. Wu, Construction of five zinc coordination polymers with 4-substituted bis(trizole) and multi-carboxylate ligands: Syntheses, structures and properties, *Polyhedron*, 2018, **155**, 223–231.

131 M.-Y. Sun and D.-M. Chen, A porous Zn(II)-based metal–organic framework for highly selective and sensitive Fe3+ ion detection in water, *Polyhedron*, 2018, **147**, 80–85.

132 S. Li, L. Lu, M. Zhu, C. Yuan and S. Feng, A bifunctional chemosensor for detection of volatile ketone or hexavalent chromate anions in aqueous solution based on a Cd(II) metal–organic framework, *Sens. Actuators, B*, 2018, **258**, 970–980.

133 N. Abdollahi and A. Morsali, Highly sensitive fluorescent metal-organic framework as a selective sensor of Mn^{VII} and Cr^{VI} anions ($MnO_4^-/Cr_2O_7^{2-}/CrO_4^{2-}$) in aqueous solutions, *Anal. Chim. Acta*, 2019, **1064**, 119–125.

134 X.-D. Zhang, Y. Zhao, K. Chen, Y.-F. Jiang and W.-Y. Sun, Water-Stable Coordination Polymers as Dual Fluorescent Sensors for Highly Oxidizing Anions $Cr_2O_7^{2-}$ and MnO_4^-, *Chem. – Asian J.*, 2019, **14**, 3620–3626.

135 B.-F. Long, M.-F. Wang, Q. Huang, X.-H. Yin, D. J. Young, F.-L. Hu and Y. Mi, A pillar-layer strategy to construct 2D polycatenated coordination polymers for luminescence detection of $Cr_2O_7^{2-}$ and CrO_4^{2-} in aqueous solution, *CrystEngComm*, 2019, **21**, 4943–4950.

136 T. Gao, B.-X. Dong, Y. Sun, W.-L. Liu and Y.-L. Teng, Fabrication of a water-stable luminescent MOF with an open Lewis basic triazolyl group for the high-performance sensing of acetone and Fe^{3+} ions, *J. Mater. Sci.*, 2019, **54**, 10644–10655.

137 P.-C. Li, L. Zhang, M. Yang and K.-L. Zhang, A novel luminescent 1D→2D polyrotaxane Zn(II)-organic framework showing dual responsive fluorescence sensing for Fe^{3+} cation and Cr(VI) anions in aqueous medium, *J. Lumin.*, 2019, **207**, 351–360.

138 P. Guo, J. Sun, Z. Xu, M. Liu, H. Li and Y. Wang, A Zn-based coordination polymer as a highly selective multi-responsive luminescent sensor for Fe^{3+} cation and $Cr_2O_7^{2-}/CrO_4^{2-}$ anions, *J. Solid State Chem.*, 2019, **273**, 62–66.

139 X.-Y. Guo, Z.-P. Dong, F. Zhao, Z.-L. Liu and Y.-Q. Wang, Zinc(II)–organic framework as a multi-responsive photoluminescence sensor for efficient and recyclable detection of pesticide 2,6-dichloro-4-nitroaniline, Fe(III) and Cr(VI), *New J. Chem.*, 2019, **43**, 2353–2361.

140 E. Khezerloo, S. M. Mousavi-khoshdel and V. Safarifard, Sensitive and selective detection of metal ions and small molecules in aqueous media using a hydrolytically stable amide-functionalized metal–organic framework, *Polyhedron*, 2019, **166**, 166–174.

141 L. Cui, Y. Li, Y. Gan, Q. Feng and J. Long, Syntheses, structure and luminescent sensing for Cr(VI)/Fe(III) of a Zn(II) coordination polymer, *J. Mol. Struct.*, 2019, **1200**, 126797.